

Efficient real-time cost management in renewable energy-powered microgrid with integrated electric vehicle charging/discharging control

Swati Sharma* , Ikbali Ali 

Department of Electrical Engineering, Jamia Millia Islamia, New Delhi, India.

*Corresponding author: swati.vashist19@gmail.com

Original Research

Received:
9 March 2025
Revised:
11 April 2025
Accepted:
29 April 2025
Published online:
1 June 2025

© 2025 The Author(s). Published by the OICC Press under the terms of the [Creative Commons Attribution License](#), which permits use, distribution and reproduction in any medium, provided the original work is properly cited.

Abstract:

The rapid proliferation of electric vehicles (EVs) has significantly escalated the strain on the public grid by exacerbating fluctuations and hindering widespread EV adoption. This paper presents a cutting-edge solution with a real-time cost optimization model tailored for AC/DC microgrid energy management. Leveraging a unique hybridization of particle-swarm optimization (PSO) and grey wolf optimization (GWO), our approach dynamically orchestrates energy flow and EV charging schedules. The model has been developed using MATLAB 2022a. Thus, a non-linear stochastic mathematical programming model optimizes EV charging and distributed energy resources (DERs) generation costs. We scrutinize our model across medium scale microgrid IEEE- 37 Node systems—via real-time digital simulator (RTDS). Our multi-level control strategy ensures both immediate response to disturbances and long-term optimization, maintaining microgrid stability. Through meticulous real-time monitoring and control, our hybrid PSO-GWO algorithm delivers superior performance, slashing costs by \$152.47 for medium scale microgrid while reducing execution time by 0.81 seconds as compared to other metaheuristic algorithms. About 36.85% of the load is absorbed by EVs, with surplus power fed back to the main grid. This comprehensive approach not only enhances the cost-effectiveness but also fosters energy efficiency, affirming the efficacy of hybrid PSO-GWO in real-time microgrid management.

Keywords: Electric vehicle; Vehicle-to-grid; Grid-to-vehicle; Particle swarm optimization; Grey wolf optimization; Electric vehicle supply equipment

1. Introduction

Microgrids stand as resilient, low-voltage networks adept at efficiently distributing energy to consumers [1]. As the demand for power surges, the integration of renewable energy resources (RERs) becomes imperative for sustainable energy provision. RERs assume a pivotal role in microgrid operations, meeting energy demands while curbing environmental impact. These microgrids encompass a diverse array of distributed energy resources (DERs) such as wind and solar power plants, combined heat and power (CHP) units, EVs and energy storage systems (ESS) [2]. Operating in either islanded or grid-connected mode, microgrids offer versatility in public services. In islanded mode, they function autonomously by drawing upon DERs whereas in grid-connected mode, they complement conventional energy sources (CESs), thereby promoting fossil fuel conservation [3]. Effective energy management stands as a linchpin for microgrid performance in real-time scenarios. Consequently, optimizing energy management within the microgrid presents formidable challenges [4] by compelling

researchers to explore a plethora of meta-heuristic algorithms aimed at enhancing microgrid efficiency.

Hybrid microgrids have become more common which have been characterized by AC/DC loads and AC/DC generation units connected to AC/DC sub-grids. This configuration reduces the need for power conversions which can improve overall microgrid efficiency [5]. They require efficient energy management within the sub-grids. Thus, optimizing the flow of power ensures the grid stability and reliability [6]. The use of RERs and EVs helps with efficient energy management [7]. The governments incentivize the adoption of EVs for a greener economy by offering tax subsidies to the consumers. The EV market is expanding rapidly because the major automotive businesses have redirected their investments towards this sector. Electric utility providers must anticipate the growing demand from EV users by investing in charging infrastructure and scaling up energy production capacity. With the surge in EV charging during peak hours, a dynamic energy management strategy becomes imperative to meet the escalating power demand [8]. For utilities, the low operational costs and ensuring system

stability have become top priority. Integrating RERs into the microgrid has become crucial for meeting energy demands, reduced emissions and ensuring seamless operations [9]. Microgrids emerge as a solution to energy and environmental disparity that adapts grid-tied and islanded installations depending on their applications [10]. However, the intermittent nature of renewable energy (RE) and fluctuating EV charging demands pose challenges in estimating energy supply and demand accurately which potentially compromise microgrid reliability [11]. Effective power management strategies must incorporate energy storage, electric vehicle supply equipment (EVSEs) demands and renewable energy (RE) production to optimize energy efficiency. Advanced control systems (ACS) and algorithms have become essential for balancing the supply and demand by minimizing energy costs and by enhancing local energy management [12]. Decentralized energy management solutions complemented by real-time feedback enable dynamic adjustments based on fluctuating energy demand and supply. AC/DC microgrids powered by REs and managed by hybrid energy management systems (EMSs) offers a sustainable approach to energy provision which requires modern control systems and decentralized management solutions to address evolving challenges effectively [13].

To achieve these objectives, the utilization of AC/DC microgrids powered by distributed energy resources (DERs) can lead to energy and cost-efficient systems. Hybrid microgrids have emerged as pivotal players in vehicle-to-grid (V2G) and grid-to-vehicle (G2V) scenarios, enabling direct interaction between EVs and the microgrid. Interconnected AC/DC sub-grids employ voltage source converters (VSCs) to regulate power flow, albeit introducing harmonics that may impact grid stability [14]. EV chargers can adversely affect electric cables and transformers, elevating losses and harmonics within the microgrid, thereby affecting EV charging/discharging performance [15]. The interconnecting converters assumes a critical role, utilizing DC-link voltage and frequency to bolster energy demand in AC/DC sub-grids while ensuring grid stability through EV charging/discharging energy management [16]. Consequently, V2G and G2V present promising avenues for establishing distributed energy storage systems (DESS) to store and release energy as needed. Effective V2G operations bolster microgrid frequency, voltage profiles, and power demand [17], offering incentives to EV owners in commercial microgrids. EV aggregators liaise with individual EV converters, orchestrating V2G or G2V operations based on grid power demand and EV charging/discharging schedules for the distributed system operator (DSO) [18]. In peak demand periods and emergencies, EV aggregators collaborate with EVs to support V2G operations within the microgrid. Thus, V2G technology garners increasing interest across diverse applications, from carbon emissions reduction to the provision of ancillary services.

In literature, a four-stage optimization algorithm has been developed for EV charging/discharging [19]. In [20, 21], authors discussed the three hierarchical control levels i.e., primary, secondary & tertiary. The primary control level controls the DERs to maintain the proper power flow within

the microgrid. The secondary level control eliminates the voltage, frequency deviations and synchronism. Similarly, the tertiary level control maintains the power flow between sub-grids. This scheme allows the microgrid to transfer power and perform efficient operations when EV has been scheduled for charging/discharging. In [22], the author discussed energy management in microgrids which encompasses various optimization techniques for addressing diverse challenges including optimal generation allocation and power scheduling. Optimal generation allocation aims to enhance microgrid performance by improving the sizing and siting of generation sources, parametric values such as power losses and generation costs. Power scheduling focuses on optimizing microgrid generator operation to minimize power losses and generation costs. Researchers have explored these optimization problems extensively as evidenced in [23, 24], which discussed optimal allocation strategies to minimize costs, emissions and other parameters. Additionally, in [25] the author introduced a stochastic multi-objective optimization model to reduce voltage deviation and operational costs in grid-connected microgrids through simulations on IEEE 34-bus test system featuring diverse energy sources and storage units. This approach ensures microgrid resilience by allowing operators to balance power quality and operational costs effectively. In [26] the author employed a modified particle swarm optimization (PSO) algorithm for real-time energy management in grid-connected microgrids focusing on efficient demand-side management through optimal battery control. Results indicate a promising reduction in operational costs by 12% over a 96-hour period, highlighting the efficacy of advanced optimization techniques in enhancing microgrid efficiency and cost-effectiveness.

In [27], the authors implemented ANN-based binary PSO and ANN-based tracking search algorithm to optimize the scheduling of microgrids within virtual power plants. Their aim was to achieve optimal power scheduling in microgrids with reduced fuel consumption, low CO₂ emissions, and enhanced system efficiency. The system performance was evaluated under diverse scenarios to assess its adaptability in emergency conditions by utilizing both trained and untrained models with actual load data. Comparative analysis against previous methodologies demonstrated the superiority of the hybrid algorithms. In [28], the author introduced a quantum-based algorithm for microgrid energy management, employing a quantum-teaching-learning-based optimization approach. This algorithm focused on optimizing energy flow in microgrids across four seasonal scenarios aiming at day-ahead scheduling based on DER availability. Results indicate significant reductions in operational costs particularly during periods of high market prices and optimized power scheduling in comparison with alternative control algorithms.

Furthermore, in [29] the authors concentrated on optimizing renewable energy microgrids in rural areas of the southern Philippines using multi-objective PSO. Their approach includes a multi-case power management strategy to design optimized microgrids considering factors such as load size, renewable energy sources and diverse objective functions.

Similarly, in [30] the authors proposed a standalone microgrid solution for rural communities utilizing renewable energy resources by evaluating the performance using differential evolution, PSO and GA algorithms which ensures the affordability of the system. These algorithms facilitate the cost-effective configurations and variability of RESs, contributing to sustainable development in remote areas. Notably, in [31] the authors applied an improved mayfly optimization algorithm (MOA) for economic emission dispatch in islanded microgrids that achieve superior results with respect to other metaheuristic algorithms in terms of reducing operational costs and emissions. The MOA algorithm contributes by minimizing the carbon footprint and achieving a balance between economic and environmental objectives. The algorithm improves the performance of the decentralized energy systems while ensuring their cost-effectiveness and sustainability with a limitation of unit commitment problem.

In [32], a lightning search algorithm (LSA) was implemented for microgrid energy management on an IEEE 14-bus system which focuses on optimizing renewable energy utilization while minimizing operational costs and emissions. The LSA handles the dynamic nature of RESs such as solar and wind which effectively balances the supply and demand within the microgrid and offers a sustainable solution for energy management. Furthermore, [33] utilized PSO and the rain flow algorithm (RFA) for day-ahead battery scheduling in a community microgrid which achieves a 40% reduction in operational costs despite uncertainties in electricity price fluctuations. The integration of these algorithms provides more accurate forecasting and decision-making by ensuring optimal battery usage while minimizing redundant costs. Finally, in [34] the authors optimized a PV microgrid using a mixed integer linear programming (MILP) model which emphasizes cost-effectiveness and versatility of microgrid in the face of geographic uncertainties. These studies collectively contribute to the ongoing efforts in optimizing microgrid energy management through diverse methodologies. The algorithm addresses unique challenges in microgrid energy management by providing the efficient solutions for diverse operational scenarios with a limitation of spinning reserve.

In [35], researchers employed the Markov decision process for power scheduling within a renewable energy-based microgrid. To address the vast decision space and complex state of the MDP, a rollout algorithm was utilized with a limitation of cost efficiency. The study in [36] implemented a memory-based GA for microgrid comprises of solar, wind and combined heat and power plants (CHP) which aims to minimize the costs through optimal energy distribution among available generation sources. In [37], authors optimized energy, heat and demand using a mathematical MILP model for minimizing operational costs with a limitation of spinning reserve and system frequency control. In [38] the authors introduced an artificial hummingbird algorithm for the optimal operation of microgrids particularly focusing on solving deterministic incentive DR programs to reduce overall costs while considering load demands in grid-connected mode. Validation of this algorithm was conducted through







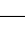
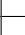
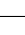
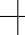






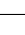







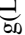

















two distinct case studies with RESs on IEEE 1548 and IEEE 1679 standards for validating the performance of PV modules and arrays and minimizing the costs for charging an EV and improving the stability of the system. Similarly, researchers in [39] tackled numerical optimization problems using the cost-effective multi-verse optimizer algorithm. By modifying the updated position mechanism in the standard multi-verse optimization (MVO) and integrating it with a sine cosine algorithm, they achieved balanced exploration and exploitation, leading to significantly improved optimization results. This approach was evaluated across 27 benchmark functions. Likewise, in [40] the authors employed MVO for power scheduling which minimizes the losses within microgrids, which has been validated on IEEE 30-bus test system and minimizes the operational costs with a limitation of non-linear loads.

The future of the power grid hinges on the integration of EVs which challenges the power quality, voltage regulation and frequency synchronization within microgrid systems. Seamlessly integrating EVs into microgrids holds promise for enhancing system flexibility and reducing electricity costs. By incorporating intelligent microgrid energy management systems with EV charging capabilities the load profiles can be flattened, peaks can be mitigated and DERs maximizes the system reliability [41, 42]. In [43], an AC microgrid with load demand-based control and onboard charging utilizes diesel generators which faces significant conversion and emissions challenges. In [44] the authors explored smart charging and flexible EV charging using power conversion methods for overcoming the phase and overloading difficulties. Optimal charging strategies leveraging variable PV power has been investigated in [45]. This paper specifically addresses the comparison between hybrid PSO-GWO with other metaheuristic algorithm for medium scaled microgrids for optimizing DERs generation costs and EV charging costs which build upon previous research efforts by targeting various performance metrics in real time environment.

By selecting metaheuristic algorithms over traditional control strategies [46] such as PSO, GA, Simulated Annealing (SA), Jaya Algorithm (JA), Teaching-Learning-Based Optimization (TLBO) and GWO, several advantages are highlighted. Metaheuristic algorithms are highly versatile and adaptable to diverse problem domains without requiring an in-depth understanding of system dynamics. This makes them well suited for applications involving nonlinear and complex systems. They are best at finding global optima within large solution spaces, where traditional control strategies often become trapped in local optima. Unlike conventional methods that rely on precise mathematical models, metaheuristic algorithms can operate effectively without explicit system equations. This is particularly advantageous in real-world scenarios where developing an accurate model may be impractical or difficult to design as shown in Table 1.

Hybrid PSO-GWO are designed to balance exploration and exploitation, enabling them to identify the most optimal solutions, especially in dynamic systems where adaptability is necessary. This balance proves beneficial when dealing with

Table 1. Comprehensive review of cutting-edge literature.

Ref.	Technique	Method mode and analysis		Generation reserve	Aim	Limitations
		Single/Hybrid	Economic/Techno-economic			
[5]	Mixed Integer Linear Programming(MILP)	single	economic		enhance microgrid operational efficiency	non-linear loads
[12]		hybrid	economic	    	reduce leveled cost of energy	intermittency of renewables
[19]		hybrid	economic	   	cost-benefit analysis for ideal storage size	spinning reserve; unit commitment problem
[22]		single	economic		minimize annual investment and operational costs	optimal sizing, type, and distribution of generators in a radial system
[27]	Linear Programming(LP)	single	techno-economic	  	maximize economic benefits, minimize annual costs	ambient conditions, demand, electricity prices, unit constraints
[29]	Cuckoo Search(CS)	single	economic	 	reduce operational costs	system reliability
[33]	Distributed Economic Model Predictive Control (DEMPC)	single	economic		optimize cost efficiency	dystem reliability
[37]	Multi-Objective Evolutionary Algorithm (MOEA)	single	economic	 	reduce switching frequency	system reliability
[39]	GA	single	techno-economic	  	optimize power rating	system reliability
[40]		single	economic	  	minimize life-cycle costs	battery state of charge limitations
[41]	PSO	single	techno-economic	 	optimize cost efficiency	system stability
[43]		single	techno-economic	 	improve stability and performance	system frequency control
[44]	Big Bang–Big Crunch algorithm (BBBC)	single	economic	 	optimize cost efficiency	system reliability
[46]	fuzzy logic– GA	hybrid	economic		predict storage lifespan, minimize costs	unit commitment problem
[47]	photovoltaic trigeneration optimization model	hybrid	economic		reduce operational costs and emissions	Intermittency of renewables
[48]	fuzzy logic–PSO	hybrid	economic	  	reduce costs and emissions	system stability
[49]	fuzzy logic–multi agent system	hybrid	economic	  	optimize cost efficiency	system stability
[50]	multiobjective grey wolf optimization (MOGWO)	hybrid	economic	  	optimize cost efficiency	unit commitment problem

changing environmental conditions and system variability. Various metaheuristics have shown substantial success in solving complex, real-world optimization problems where traditional control strategies may fall short. Among these, GWO stands out for providing superior solutions for cost-effective EV charging/discharging management. Its simplicity, robustness and fast convergence make it well-suited to handle uncertainties during peak and off-peak hours, achieving optimal solutions in shorter computation times compared to other metaheuristic algorithms. This efficiency establishes GWO as a preferred method for real-time EV charging/discharging cost optimization.

However, the literature extensively explores EV charging scenarios employing various control techniques integrated with multi-objective PSO within distribution networks as detailed in [47]. Reference [51] presents energy management strategies for EVs including optimized charging schemes and travel patterns, utilizing both PSO and GA. In reference [48], the author examines optimal scheduling for time-shiftable loads through DR programs, employing advanced algorithms such as the Cuckoo Search Algorithm (CSA) and Symbiotic Organism Search (SOS). These studies collectively aim to achieve optimal scheduling of EV charging patterns and minimize the cost of EV charging [49] with strategies often leveraging PV systems as the primary source of power generation. In this study, the proposed hybrid PSO-GWO scenario for EV charging/discharging incorporates RESs to ascertain the most optimal cost for both V2G and G2V support. Moreover, by deliberately managing EV charging/discharging during peak and off-peak hours through hybrid PSO-GWO, the exploration capabilities of PSO with the exploitation capabilities of GWO achieve faster convergence as compared to other algorithms. However, the hybrid PSO-GWO algorithm tends to converge prematurely when locating charging stations (CSs) for EV charging more quickly which leads to suboptimal solutions without fully exploring the nearby CS search space. The hybrid PSO-GWO algorithm offers a balanced exploration of the search space and nearby CSs for EV charging/discharging avoiding local optima in V2G or G2V operations within the microgrid. This results in optimized costs, reduced computational time, improved stability and reliability.

In previous studies, the researchers employed various metaheuristic algorithms and control techniques integrated within microgrid framework which facilitates the grid stabilization and cost minimization through strategic EV charging/discharging which effectively mitigates power fluctuations. However, these approaches compromise the system reliability, necessitating a balanced strategy to ensure both performance and robustness of the system. Thus, focusing on the limitations of the previous studies, the manuscript discusses the strategic real-time EV charging/discharging scenario using hybrid PSO-GWO algorithm for a reliable, stable and cost-efficient system in V2G and G2V framework. Thus, the major contributions of this manuscript are distributed into following points:

- Integrating RE systems with EVs offers twofold benefits: It mitigates harmful emissions while improving resource efficiency by harnessing the energy storage

capabilities inherent in EVs.

- This synergy enables the surplus RE produced during peak generation periods to be stored in EV batteries and subsequently deployed during times of heightened demand, thus diminishing reliance on conventional, fossil fuel-based power generation.
- The deployment of a hierarchical control system, coupled with integrated circuits (ICs), voltage source converters (VSCs) and EV aggregators, proficiently oversees the charging/discharging of EVs within an AC/DC microgrid powered by DERs. This holistic strategy not only optimizes generation costs but also ensures the effective utilization of RE, thereby fortifying system reliability and sustainability.
- Employing a hybrid PSO-GWO algorithm, integrated with MATLAB and RTDS, streamlines the optimization of EV charging (G2V) and generation costs within the microgrid. The incorporation of hybrid PSO-GWO technique enhances system performance by maximizing grid stability and minimizing evaluation time ensuring seamless operation in real-time scenarios.
- Furthermore, the bidirectional power flow capability of EVs supports the additional services like frequency regulation, spinning reserves and load balancing which contributes to overall stability, resilience, efficiency and optimized generation costs of the microgrid.

The paper is organized as follows: Section 2 presents system architecture and mathematical modelling which discusses the modelling of PV array, wind power plants constraints, combined heat and power constraints, EV charging scheme with different control arrangements, SOC estimation and their objective cost function. Section 3 discusses the hybrid PSO-GWO methodology and their integration with microgrids in real time environment for better performance and obtaining the optimized costs. Section 4 discusses the results which optimizes the generation costs and EV charging costs for medium scale microgrid (IEEE-37 node test feeder) integrated with RTDS for improving its performance and evaluation time. Section 5 discusses the conclusions that the hybrid PSO-GWO outperforms all other metaheuristics algorithms in less evaluation time and reduced generation and EV charging costs in real time environment.

2. System architecture and mathematical modelling

The AC/DC microgrids with EV charging infrastructure requires a comprehensive system architecture for efficiently managing the power flow, ensuring the stability and optimizing energy usage. At its core, the AC/DC microgrid architecture encompasses various components such as power converters, energy storage systems, renewable energy sources and grid interconnections as shown in Fig. 1. In this section, the AC/DC microgrid combined with DERs using RSCAD paired with RTDS. The interconnecting converter and AC microgrid have a step-size of $3.72 - 10 \mu s$ in sub-step environment and $50 \mu s$ in main-step environment. In sub-step

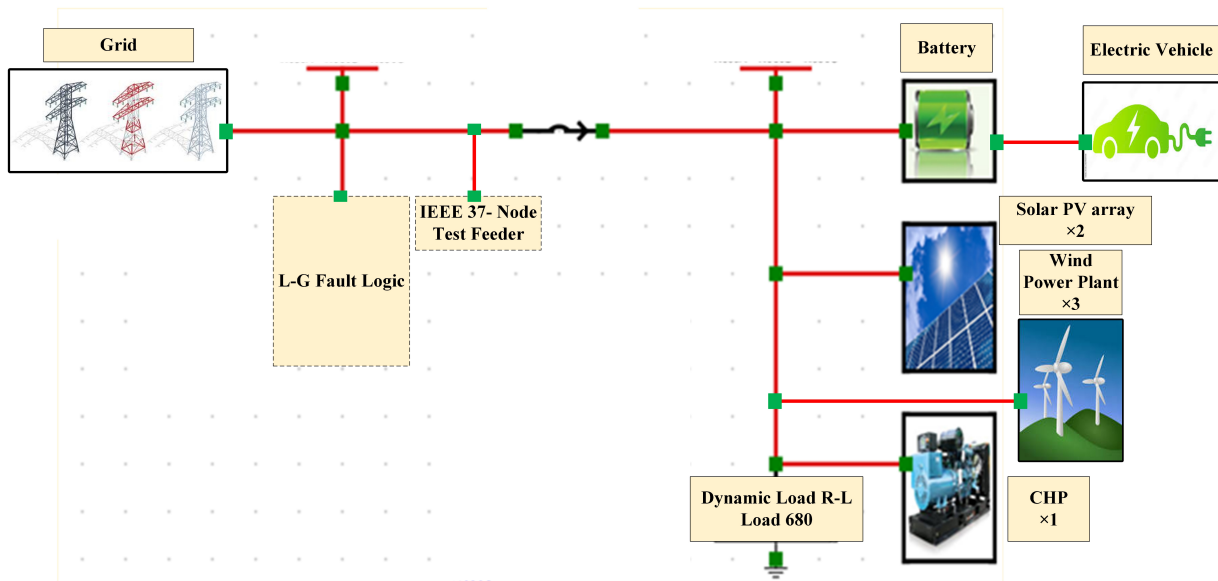


Figure 1. Representation of IEEE-37 node microgrid.

environment IC-VSC and PV boost converters have been designed using resistive switching model whereas bidirectional DC/DC converters have been designed by average model. In the main step environment, the average model has been designed by integrating DER converters. To distribute the burden on three cores of the RTDS, two sub-step environment and main-step environment constructs the draft case of the microgrid using C-builder which provides user to build new components in the RSCAD by importing control system model from MATLAB 2022a to RTDS. It is also used to build and implement microgrid average and control system models specifically for power converters.

2.1 PV array dynamics

Some of the places worldwide is ample with sunlight. Solar energy emerges as a plentiful and dependable resource accessible for extended periods throughout the year. PV panels adroitly harness this energy by transforming it into DC electrical power. For seamless integration of PV panels into existing electrical grids, the inverters assume a critical role in converting the DC power into AC power. The output of a PV plant remains susceptible to diverse fluctuating factors such as solar radiation and ambient temperature by rendering its electrical output variable. To achieve precise forecasts of energy generation, stochastic modeling becomes indispensable. Through the analysis, the stochastic PV array model can proficiently estimate the electrical energy output of the PV plant by furnishing invaluable insights for effective energy planning and management. The current output of a single PV array model (I_{PV_cell}) can be calculated using Eq. (1):

$$I_{PV_cell} = I_{pg} - I_{Rev} * e^{\left\{ \left(\left(\frac{V+R_s I}{\eta V_t} \right) - 1 \right) - \left(\frac{V+R_s I}{R_p} \right) \right\}} \quad (1)$$

where I_{pg} is photogenerated current, I_{Rev} is reverse current, η represent ideality factor of the diode, R_s & R_p are series resistance and shunt resistance respectively. These cells are connected in series to form the module and similarly these

modules continue to form PV array. The maximum power of the PV array can be calculated through Eq. (2):

$$P_{MPPT} = V_{MPPT} * I_{MPPT} \quad (2)$$

where, V_{MPPT} and I_{MPPT} are maximum power point voltage and current. The PV array is connected to the DC sub grid through boost converter with breaker and startup control logic. The boost converter is essential for efficiently increasing the DC voltage generated by the PV array for ensuring the optimal power transfer to the sub-grid. The breaker serves as a safety mechanism by enabling isolation of the PV array from the sub-grid during maintenance or in the event of faults. The startup control logic initiates and regulates the operation of the converter for ensuring smooth and reliable system at the time of energy production. Also, for extracting maximum power from the PV array MPPT technique has been employed. I-VSC is the most vibrant part of the AC/DC microgrids which manages the balance between the two sub grids consisting of outer power controller, middle voltage controller and inner current controller. The d-q frame for I-VSC control works with modified droop characteristics [15] for active control, reactive power control and frequency control.

Where ω_{inst} , ω_{ref} are instantaneous and reference frequency in rad/sec which has been provided in Eqs. (3-4),

$$\omega_{inst} = \omega_{ref} - D_p^{IC(P-d^{ref})(K_p^{IC}+s*K_d^{IC})} \quad (3)$$

$$V_{inst} = V_d^{ref} = V^{ref} (f - D_q^{IC(q-q^{ref})(K_p^{IC}+s*K_d^{IC})}) \quad (4)$$

where, $D_p^{IC(P-d^{ref})(K_p^{IC}+s*K_d^{IC})}$ is IC-VSC and $V^{ref}(f - D_q^{IC(q-q^{ref})(K_p^{IC}+s*K_d^{IC})})$ is Q (reactive power) -V (voltage) droop coefficient. 'f' is the frequency, ' D_p ' is the droop coefficient, 'd' is the direct axis, 'q' is the quadrature axis, d^{ref} is the reference direct axis and qref is the reference quadrature axis.

K_{pc}^{IC} is IC-VSC proportional coefficient power control loop

& K_d^{IC} is derivative coefficient in power control loop at grid converter side. The reference current in PV array can be calculated through d-q axis which can be expressed in Eqs. (5-6),

$$I_d^{ref} = (V_d^{ref} - V_d)(K_{PV}^{IC} + \frac{K_i^{IC}}{S} - \omega C_f V_q) \quad (5)$$

$$I_q^{ref} = (V_q^{ref} - V_q)(K_{PV}^{IC} + \frac{K_i^{IC}}{S} - \omega C_f V_d) \quad (6)$$

where, V_d^{ref} and V_q^{ref} are reference voltage control loop for d-q component, K_{PV}^{IC} is IC-VSC voltage control loop, ' C_f ' is the capacitive frequency, V_d is the Voltage at direct axis, V_q is the voltage at quadrature axis, K_i is the integral IC-VSC constant. The inner current controller can be expressed by the following equations (7-8):

$$V_d^{ref} = (I_d^{ref} - I_d)(K_{PC}^{IC} + \frac{K_i^{IC}}{S} - \omega L_f I_q) \quad (7)$$

$$V_q^{ref} = (I_q^{ref} - I_q)(K_{PC}^{IC} + \frac{K_i^{IC}}{S} - \omega L_f I_d) \quad (8)$$

where, K_{PC}^{IC} and K_i^{IC} are IC-VSC proportional and integral coefficient in the current control loop. ' L_f ' is inductive frequency, ' I_d ' is current at direct axis and ' I_q ' is the current at quadrature axis. The secondary controller (SC) monitors the DC bus voltage and tunes the reference value to reduce the deviations occurred during operation with droop-controlled converters [15]. The primary objective of this hierarchical controller is to maintain the nominal voltage condition of the microgrid. The DC bus reference voltage can be tuned using PI controller and can be expressed in Eq. (9),

$$V_{DC}^{ref} = (\frac{K_P^{SC} + K_i^{SC}}{S})(V_{DC}^{rated} - V_{DC}^{inst}) \quad (9)$$

where, V_{DC}^{rated} and V_{DC}^{inst} are rated and instantaneous DC bus voltage. K_P^{SC} and K_i^{SC} are proportional and integral coefficients of secondary controller [16]. The PV array power generation limit and the power balance equation can be written as Eqs. (10-11), where P_i is the maximum demand of PV grid.

$$P_{PV}(t) \leq P_{\max, PV} \quad (10)$$

$$P_{Grid}(t) + P_{PV}(t) = P_i \quad (11)$$

where, $P_{\max, PV}$ is the maximum PV power; $P_{PV}(t)$ is the maximum PV power at time (t); $P_{Grid}(t)$ is the grid power.

2.2 Wind power plant (WPP) and combined heat and power (CHP) constraints

The (P_{WPP}) power generated by a WPP is dependent on wind speed. There is a maximum power P_{\max} that can be generated at a given time as shown in Eqs. (12-13),

$$P_{WPP}(t) \leq P_{\max} \quad (12)$$

$$P_{WPP}(t) \geq P_{\min} \quad (13)$$

where, P_{\min} is the minimum power generated in WPP. Similarly, the CHP system generates electricity and heat. It

has a maximum electricity generation capacity $P_{CHP,elec}$ at any time as shown in Eq. (14),

$$P_{CHP,elec}(t) \geq P_{\max,elec} \quad (14)$$

The power balance Equation for grid, wind plant and CHP can be calculated as (15),

$$P_{Grid}(t) + P_{WPP}(t) + P_{CHP}(t) = P_i \quad (15)$$

These constraints ensure that the total power from the grid, WPP and CHP system meets the total demand. The WPP and CHP operate within their generation limits, and the CHP system operates within its combined capacity for electricity and heat generation.

2.3 EV state-of-charge (SOC) estimation

SOC refers to the amount of energy stored in EV battery as a percentage of its total capacity. It indicates the available driving range and is crucial for efficient trip planning. Monitoring SOC helps drivers avoid running out of power for promoting a smoother and more reliable journey. Moreover, maintaining the optimal SOC levels prolongs battery life. As EV technology advances, the accurate SOC readings, which become increasingly important for enhancing driving experience and fostering widespread adoption of EVs. The SOC estimation for EVs and EVSEs per trip can be calculated through Eq. (16),

$$SOC_{trip} = \sigma \frac{M}{M_{\max}} \quad (16)$$

where, ' σ ' is the driving efficacy during EV charging/discharging, ' M ' is the distance travelled by EV per trip and M_{\max} is maximum distance travelled by the EV for the whole day. The SOC during EV charging (SOC_{ch}^{EV}) can be calculated through Eq. (17), and EV discharging (SOC_{disch}^{EV}) can be calculated through Eq. (18),

$$SOC_{ch}^{EV} = SOC_I^{EV} + C_{ch} * \epsilon_{ch} * T_{ch}^{EV} \quad (17)$$

$$SOC_{disch}^{EV} = SOC_I^{EV} + C_{disch} * \epsilon_{disch} * T_{disch}^{EV} \quad (18)$$

where, SOC_I^{EV} is EVs initial stage, C_{ch} and C_{disch} are EV battery charging/discharging efficacy and its performance, ϵ_{ch} and ϵ_{disch} are the EV charging/discharging rate, T_{ch}^{EV} and T_{disch}^{EV} are dedicated scheduling for EV charging/discharging process. The battery SOC constraint for EV charging/discharging is shown in Eq. (19),

$$0 \leq SOC_I^{EV} \leq SOC_{\max} \quad (19)$$

2.4 EV power equation

The EV control scheme plays a pivotal role in managing the growing demand for sustainable transportation. This scheme employs sophisticated algorithms and smart technologies to optimize charging operations by ensuring a harmonious balance between grid stability, user convenience and energy efficiency. By leveraging real-time data analysis, it dynamically adjusts charging rates based on grid load, renewable energy availability and user preferences. This intelligent system minimizes peak loads, fosters grid

resilience and encourages off-peak charging by reducing electricity costs and carbon emissions which support grid stability during fluctuations.

In this segment, the EVs can be implemented in two modes: dispatched mode and voltage droop control mode. In normal conditions, the dispatched control mode has been used by scheduling EV for charging/discharging at EVSEs. In case of EVs discharged battery energy storage system (BESS), the voltage droop control is used to maintain the DC bus voltage.

In the dispatched mode, the constant power flow has been achieved by controlling the inductor current using the PI controller. In voltage droop control mode, each EV controls the DC bus voltage using cascade PI control loops which gives power-sharing in accordance with their power rating [22]. Droop controlled in DC sub grid can be calculated using Eq. (20),

$$V_{DC}^{inst.Bus} = V_{DC}^{ref} - I_{DC}R_{droop} \quad (20)$$

where, $V_{DC}^{inst.Bus}$ and V_{DC}^{ref} are DC bus instantaneous and reference voltage, I_{DC} is the DC bus current for EV converter and R_{droop} is the droop coefficient for EV converter. During dispatchable mode the current reference depends upon the power reference and can be calculated in equation (21),

$$I_{EV}^{ref} = \frac{P_{ref}}{V_{DC}} \quad (21)$$

where, I_{EV}^{ref} and P_{ref} are the reference current and power for EV respectively. During voltage-droop mode the current reference can be calculated through Eq. (22),

$$I_{EV}^{ref} = (V_{DC}^{ref} - V_{DC} - I_{DC} * R_{droop}) \left(K_P^{EVV} + \frac{K_I^{EVV}}{S} \right) \quad (22)$$

where, K_P^{EVV} and K_I^{EVV} are proportional and integral coefficient in voltage control loop for EV converter. A large value of the virtual resistor provides better load sharing but produces more voltage deviation. Droop coefficient (D_p) is the ratio of maximum deviation in DC bus voltage as shown in Eq. (23), when maximum power is fed back to microgrid. To have proportional power-sharing the product of power droop coefficient (D_p) and the maximum power of all EV unit must be equal.

Inductor current control [42] in DC/DC converter can be calculated through Eq. (23),

$$D_p = \frac{(I_{EV}^{ref} - I_{EV})(K_P^{EVC} + \frac{K_I^{EVC}}{S})}{V_{DC}} \quad (23)$$

where, K_P^{EVC} and K_I^{EVC} are proportional and integral coefficient in current control loop for EV converter.

$$P_i = \sum SOC_{ch}^{EV} - SOC_I^{EV} * D_p + V_{MPPT} * I_{MPPT} \quad (24)$$

where, P_i is the total power generated by the available DERs calculated in Eq. (24).

2.5 Cost function

The microgrid encompasses a diverse array of variable load and intermittent generation sources, such as PV arrays, diesel generator (DG) units and EV batteries. Due to the dynamic nature of demand and fluctuating power generation, the primary objective is to efficiently meet the demand load requirements. Numerous strategies exist for allocating energy among DERs with a paramount focus on minimizing EV charging costs for the optimal energy management approach within the microgrid ecosystem.

$$C_j = \beta_j * P_j^2 + \alpha_j * P_j + \delta_j \quad (25)$$

where, β_j , α_j and δ_j are the cost coefficients of the micro-grid. C_j represents the total cost. P_j represents the power in j^{th} generation in MW/hour calculated in Eq. (25). A quadratic cost function is employed for each generation unit to effectively minimize overall generation expenses. The total cost incurred in each hour is determined by summing up the costs associated with all DERs utilized during that period. The primary objective remains the fulfillment of load requirements through power generation at the lowest possible cost. Additionally, this approach assumes that generation will consistently match the load demand.

2.6 Equality constraints

For seamless implementation, it is crucial to ensure that the generated power consistently exceeds or at least matches the demand power at any given moment. DERs fall short of meeting the demand, thus the deficit is supplemented by drawing from the utility grid. In this study, we operate under the assumption that the available load capacity consistently meets the demand, rendering external energy procurement from the utility grid unnecessary. This can be formulated in Eq. (26):

$$\sum_{i=1}^{DER} P_i = P_t \quad (26)$$

where, P_i is the total power generated from available DERs, P_t is the power demanded at a particular hour of the day. The hourly generated power is determined by aggregating the power outputs of all generation units within the microgrid. This study examines medium scale microgrid configurations, each characterized by varying number of generation units. It is imperative that each generation unit operates within its specified limits. This operational constraint can be succinctly represented in Eq. (27):

$$P_{i \min} \leq P_i(t) \leq P_{i \max} \quad (27)$$

where, $i = 1, 2, \dots, M_{DER}$ and $t = 1, 2, 3, \dots, 24$. This equation stipulates that, at time 't', the power output from any generation unit must consistently fall within a predefined range. ' $P_{i \min}$ ' denotes the minimum allowable power output for any generation unit, typically set to zero, while ' $P_{i \max}$ ' represents the maximum power output or total demand achievable based on the rated power capacity. These values effectively delineate the lower and upper bounds by forming the boundary for the generation vector.

2.7 Objective function

Each generation unit serves as a decision variable in the pursuit of cost minimization. Consequently, the scale of microgrid dictates the variance in decision variables. The total EV charging costs is computed as the summation of costs incurred by all utilized generation units. Employing equality constraints, the energy management system strives to harmonize generation power with the demanded load. Hence, the overarching objective of the optimization algorithm is to leverage generated power from available units by minimizing the overall EV charging costs in V2G and G2V scenarios. To address this power scheduling challenge, the optimization function outlined in Eqs. (28-29) [51] must be tackled.

$$\text{Minimize } C(j) = \sum_{j=1}^{\text{DER}} \beta_j * P_j^2 + \alpha_j * P_j + \delta_j \quad (28)$$

$$\sum_{i=1}^{\text{DER}} P_i = P_t \quad (29)$$

Indeed, ensuring that the generated power remains within the specified range poses a significant challenge in optimization problems. To effectively manage this constraint, introducing a penalty function proves to be a viable solution. By incorporating a penalty function, the optimization process can be guided in a more balanced manner, facilitating the achievement of optimized outcomes while adhering to operational constraints. The equation for the objective function incorporating the penalty function, as outlined in [45] and Eq. (30),

$$C(j) = \sum_{j=1}^{\text{DER}} [\beta_j * P_j^2 + \alpha_j * P_j + \delta_j] + P_f \sum_{i=1}^{\text{DER}} P_i \quad (30)$$

where, $C(j)$ represents the total cost in dollars, β_j , α_j and δ_j are the cost coefficients and P_f is the penalty factor that maintains the balanced equations for the microgrid.

3. Real-time cost optimization for EV charging/discharging using hybrid PSO-GWO algorithm

This section elucidates the hybridization of PSO and GWO algorithm and its efficacy in achieving optimized generation costs for microgrids and EV charging costs. It delves into a cost-effective variant of hybrid PSO-GWO algorithm by examining it with other metaheuristic algorithms for minimizing the costs within microgrid.

PSO was proposed by Dr. James Kennedy and Dr. Russell Eberhart in 1995. They introduced the concept while working at the Kennedy Space Centre, NASA, USA, inspired by the social behaviour of birds flocking and fish schooling. It iteratively updates a group of candidate solutions (particles) based on their own experience and the best solution found by the swarm aiming to converge towards optimal solutions. GWO is a metaheuristic algorithm inspired by the social hierarchy and hunting behaviour of grey wolves. The algorithm was introduced in 2014 by Mirjalili et al., it divides the population into alpha, beta and delta wolves

representing solutions. The wolves iteratively update their positions based on alpha leadership, beta and delta and prey proximity. GWO effectively balances exploration and exploitation by demonstrating competitive performance in solving optimization problems across various domains.

The hybrid PSO-GWO algorithm combines the strengths of two prominent optimization techniques by leveraging their complementary features to enhance search efficiency and solution quality. PSO is inspired by the collective behaviour of bird flocks and fish schools where particles in the search space iteratively adjust their positions based on their own experience and the best solution found by the swarm. On the other hand, GWO mimics the social hierarchy and hunting behaviour of grey wolves by dividing the population into alpha, beta, and delta wolves to exploit exploration and exploitation capabilities effectively.

In the hybrid PSO-GWO algorithm, the particles interact within the swarm according to PSO principle, while the global best solution guides their movement. At the same time, the wolf pack hierarchical structure and hunting strategy from GWO provide additional guidance for exploration and exploitation. By hybridizing PSO-GWO algorithm, it aims to strike a balance between exploration and exploitation by ensuring robust convergence towards optimal solutions and maintaining the computational efficiency. Through hybridization, the PSO-GWO algorithm inherits the ability of PSO to quickly explore the search space and the exploitation capability of GWO to refine solutions locally. This synergistic combination enables the algorithm to effectively tackle complex optimization problems like optimizing microgrid generation costs by integrating EVs with various IEEE bus standards using pattern recognition and machine learning. The universal steps for solving a problem using the hybrid PSO-GWO algorithm are as follows:

- Step 1:** Initialize the population of particles representing candidate solutions and the positions of the wolves in the search space.
- Step 2:** Evaluate the fitness of each particle and wolf position using the objective function associated with the problem being solved.
- Step 3:** Update the personal best positions of particles and the global best position found by the swarm.
- Step 4:** Update the velocity and position of each particle using the PSO equations by incorporating personal and global best positions.
- Step 5:** Update the positions of alpha, beta and delta wolves using the GWO equations by considering the hierarchy and hunting behavior.
- Step 6:** Combine the movements of particles and wolves by potentially adjusting the weights or proportions of PSO and GWO influences.
- Step 7:** Check convergence criteria such as maximum iterations or reaching a satisfactory solution.
- Step 8:** If convergence criteria are met, terminate the algorithm; otherwise, return to step 2.

Step 9: Determine the best solution found by the algorithm as output.

These steps iterate until a termination condition is met i.e., when a satisfactory solution will be obtained, or a maximum number of iterations has reached. The hybridization of PSO and GWO allows for a balanced exploration and exploitation of the search space which enhances the algorithm effectiveness in finding optimal solutions to various optimization problems. Adjustments to parameters and strategies may be made to improve performance for specific problem instances. The flow chart of hybrid PSO-GWO algorithm.

Optimizing EV charging costs is a critical concern amid the transition towards sustainable transportation. The hybrid PSO-GWO algorithm offers a promising avenue to address this challenge effectively. By integrating the strengths of PSO global search capability and GWO hierarchical exploration, the hybrid approach can navigate the complex search space of charging schedules and energy tariffs efficiently. The algorithm optimizes EV charging schedules by considering factors such as battery SOC, microgrid charging loads and user preferences. PSO adjusts charging rates and time scheduling for EV charging iteratively by minimizing the costs and ensuring timely completion of charging tasks. Meanwhile, GWO dynamically adapts the charging strategy by leveraging the hierarchical structure to balance exploration and exploitation of the solution space effectively. Meanwhile, the real-time digital simulator provides a virtual environment to simulate various charging scenarios for medium scaled microgrids integrated with EVs and assess their impact on grid performance and user costs. By integrating RTDS enables rapid prototyping and testing of charging strategies in a risk-free environment by allowing for the evaluation of different optimization objectives and constraints. Additionally, real-time simulation facilitates the implementation of adaptive charging algorithms that respond to sudden changes in grid conditions or user requirements. The hybridization of PSO-GWO can be modelled by the following equations (31-47);

$$\alpha_j = \alpha_{ch} + \alpha_{disch} \quad (31)$$

$$\beta_j = \beta_{ch} + \beta_{disch} \quad (32)$$

$$\delta_{ch} = \frac{\alpha_{ch}}{\beta_{ch}} \quad (33)$$

$$\delta_{disch} = \frac{\alpha_{disch}}{\beta_{disch}} \quad (34)$$

Thus, δ_j can be calculated through eq (35),

$$\delta_j = \sum_{i=1}^{EV_{ch}} \sum_{j=1}^{EV_{disch}} \alpha_j * \beta_j \quad (35)$$

where, α_j , β_j and δ_j are the cost coefficients integrated with EVs for charging/discharging as shown in Eqs. (31-35).

α_{ch} , β_{ch} is the EV customer behaviour while charging, δ_{ch} and δ_{disch} is the peak load demand utilized for EV charging/discharging. α_{disch} , β_{disch} is the EV customer behaviour while discharging.

Thus, optimizing the operation of DERs along with EV charging/discharging minimizes the costs. It involves a complex interplay of factors such as electricity prices, DER capacities, EV battery constraints and user requirements using hybrid PSO-GWO. The integration of hybrid PSO-GWO with real time environment has been modelled. The equations of hybrid PSO-GWO are as follows:

$$P_{j+1} = \sigma * P_j + C * r_1 (P_j - SOC_i) + (SOC_{disch}^{EV} - SOC_i) \quad (36)$$

$$SOC_{i+1} = SOC_i + P_{j+1} \quad (37)$$

where, P_{j+1} represents EV charging/discharging rate at i^{th} iteration, SOC_i is the SOC of EV at i^{th} iteration. The mean waiting time (W_t) for EV charging/discharging can be calculated using Eq. (38),

$$W_t = \beta_j - 1 \prod_0^{initial} [\delta_j]^{-2} \quad (38)$$

Thus, determining the alpha, beta and delta wolves using Eqs. (39-46)

$$A = 2br_1 - b \quad (39)$$

$$C = 2r_2 ; a = 2r_3 \quad (40)$$

where, t is the current iteration, A , C are the coefficient vectors of grey wolf; r_1 , r_2 and r_3 are random uniformly distributed between 0 and 1 and a is linearly decreasing coefficient from 2 to 0.

1. Alpha, beta, and delta wolves: GWO maintains three special wolves in equations (41-43);

$$\vec{Z}_1 = \vec{Z}_{\alpha} - A * SOC_i \quad (41)$$

$$\vec{Z}_2 = \vec{Z}_{\beta} - A * SOC_i \quad (42)$$

$$\vec{Z}_3 = \vec{Z}_{\delta} - A * SOC_i \quad (43)$$

a. Alpha wolf: The wolf with the best fitness value can be obtained from equation (44);

$$\vec{Z}_{\alpha} = SOC_{i+1} - \vec{Z}_1 \cdot r_1 |C \cdot \vec{Z}_1 - SOC_{i+1}| \quad (44)$$

b. Beta wolf: The wolf with the second-best fitness value in equation (45);

$$\vec{Z}_{\beta} = SOC_{i+1} - \vec{Z}_2 \cdot r_2 |C \cdot \vec{Z}_2 - SOC_{i+1}| \quad (45)$$

c. Delta wolf: The wolf with the third-best fitness value in equation (46);

$$\vec{Z}_{\delta} = SOC_{i+1} - \vec{Z}_3 \cdot r_3 |C \cdot \vec{Z}_3 - SOC_{i+1}| \quad (46)$$

Thus, alpha, beta and delta wolves are participating in the hunting process for obtaining the best cost for EV charging/discharging.

Updating Positions: All other wolves in the population adjust their positions based on the positions of the alpha, beta, and delta wolves. This mimics the social behaviour of wolves where other wolves in the pack follows the leaders. Exploration and Exploitation: GWO balances exploration (searching for new, potentially better solutions) and exploitation (focusing on the best-known solutions) by using

mathematical equations to guide the wolves' movements. The generated power costs for EV charging/discharging using hybrid PSO-GWO are formulated in Eq. (47):

$$\sum_{i=1}^{DER} P_j = \frac{\vec{Z}_\alpha + \vec{Z}_\beta + \vec{Z}_\delta}{3} + W_i * SOC_{trip} \quad (47)$$

Iterative Process: The algorithm continues through multiple iterations or generations. In each iteration, the positions of the wolves are updated based on the positions of the alpha, beta, and delta wolves, and the fitness of the new solutions has been evaluated by finding a suitable search space for best solution using PSO routine.

The algorithm tries to minimize charging during peak electricity demand times to reduce costs. The algorithm takes decisions about when and where to charge/discharge the EVs by considering arrival time, departure time and the peak demand. This system will efficiently manage the EVs within a microgrid and reduce the operational expenses. The EV charging/discharging process within the microgrid minimizes the EVs charging costs at EVSEs and power utilized by EVs for charging using hybrid PSO-GWO. This system calculates an optimized cost using equation (30) and input price profiles provided in Algorithm 1 pseudo code. It finds the most cost-effective path for EVs charging/ discharging. This implies that EVs have multiple options for charging and the system needs to decide which EVSE will be used by EVs.

Thus, hybrid PSO-GWO determines a desired search space i.e., nearest EVSEs with respect to the EVs and then simulates a pack of wolves consisting of alpha, beta and delta

wolves for EV charging/discharging. These represent the lead wolves in the pack. The algorithm initializes a population of wolves which represents a potential solution for V2G and G2V support. The alpha, beta, and delta wolves determine fitness values.

The alpha wolf shows the best solution, the beta wolf shows the second-best solution, and the delta wolf shows the third best solution. Each wolf updates its position based on the positions of the alpha, beta and delta wolves in the form of EVs data. This step is designed to balance exploration and exploitation. The new position of a wolf is calculated using a search equations (44-46) that involves the positions of the alpha, beta and delta wolves using equations (41-46) and the PSO determines the solution space using equations (36-37).

The equation guides the search towards potentially better solutions. If EVs moves outside the search space boundaries, it must be brought back inside the boundaries using suitable boundary-handling techniques for charging. After updating the positions, the alpha, beta and delta wolves will be redefined based on their new fitness values in the form of SOC. The algorithm repeats the steps until a stopping criterion has been met. Common stopping criteria includes a maximum number of iterations that reaches a specific fitness threshold or a time limit.

Through this hybridization, the algorithm can find near-optimal charging schedules that minimizes the costs for EV owners while considering constraints such as charging station availability and grid demand. Such optimization not only reduces charging expenses for users but also pro-

Algorithm 1 pseudo code: Function handling for EV charging/discharging using hybrid PSO-GWO

Input: EV Profiles

Output: EV Scheduling for charging or discharging

Initializing the number of EVs.

Updating the EVs data (select EV having minimum waiting time.

If [new vehicle plugged in] → [set the charging demands]

Else

 Update the nearest EVs data

Endif

Initializing the load parameters SOC, α , β and δ

Assigning the initial values - \vec{Z}_1 , \vec{Z}_2 , \vec{Z}_3

Determining the load parameters with respect to the fitness function for charging or discharging of EV.

Update the best values - \vec{Z}_α , \vec{Z}_β , \vec{Z}_δ , P_{j+1} , SOC_{i+1}

If $SOC_{EV} < SOC_{BDT}$

 EV is scheduled for the charging

Endif

If $SOC_{EV} > SOC_{BDT}$

 EV is scheduled for discharging

Endif

EV→MG: Microgrid updates the EV charging/discharging process with other DERs within medium scale microgrid and determines the performance in real-time environment.

motes grid stability by distributing charging loads intelligently. Overall, the hybrid PSO-GWO algorithm interacts with RTDS, allowing it to receive system state information for performing optimization iterations and adjusting system parameters as needed during simulation runs as shown in Fig. 2. It provides a great potential in enhancing the affordability, performance and efficiency of EV charging infrastructure by facilitating the widespread adoption of EVs in the transition towards sustainable mobility and obtaining minimized generation costs in less evaluation time.

4. Results and discussion

In this section, experimental and simulation descriptions have been provided. Furthermore, the performance of the

proposed algorithm is assessed by implementing it across a medium scale microgrid model using RTDS as shown in Fig. 3.

4.1 Experimental setup and data set description

The hybrid PSO-GWO has been implemented using MATLAB 2022a and these cost parameters were incorporated in hierarchical AC/DC microgrid model using Real time digital simulator (RTDS Technologies NovaCor Model-1A) as shown in figure 3. These experiments were executed on a computer with a Windows 10 64-bit operating system specification, Intel (R) core (TM) i7 and 16 GB RAM. The algorithms have been implemented using MATLAB and cost-optimized EV aggregator parameters which were

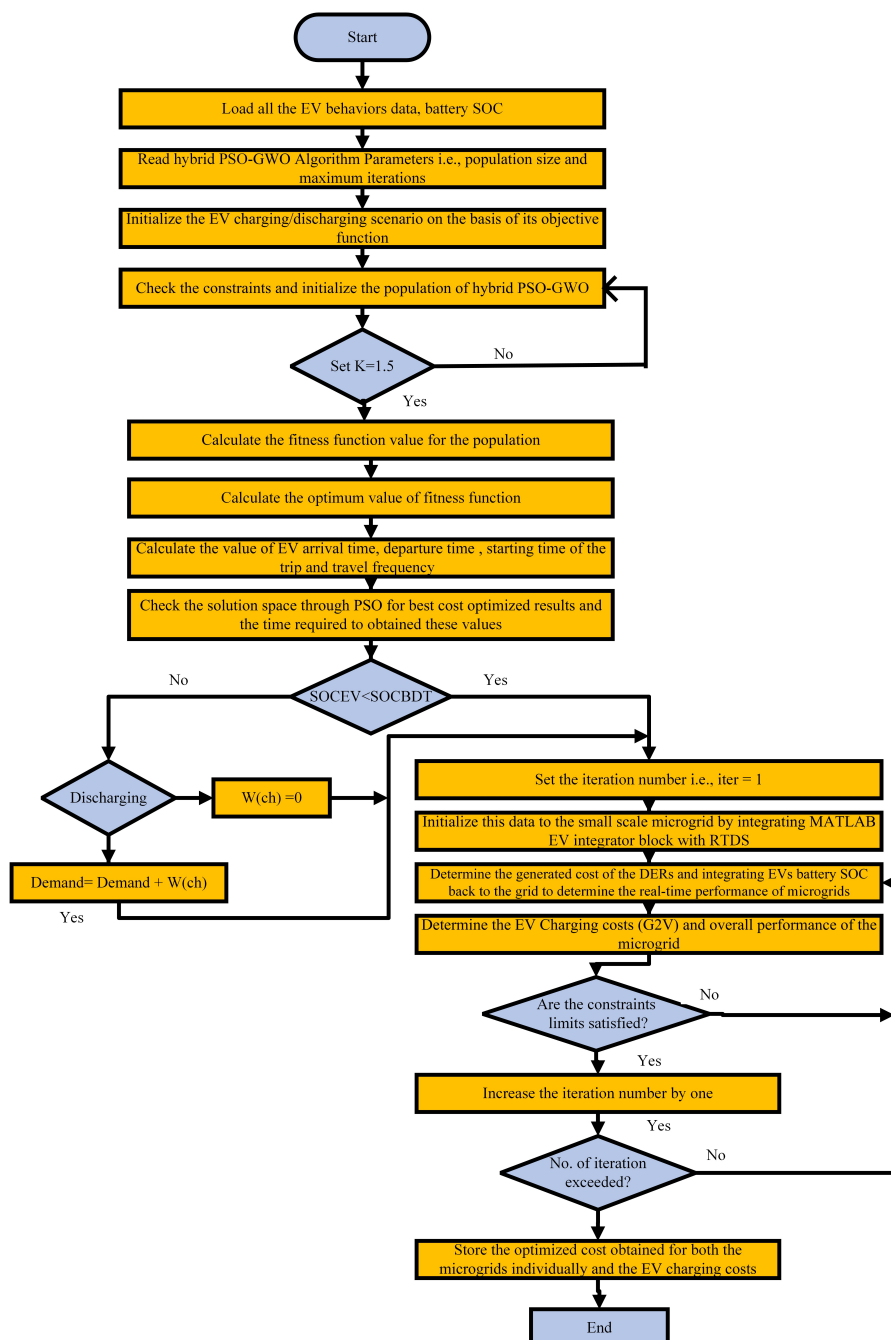


Figure 2. Flow chart of real time cost optimization of DERs generation costs and EV charging costs using hybrid PSO-GWO.

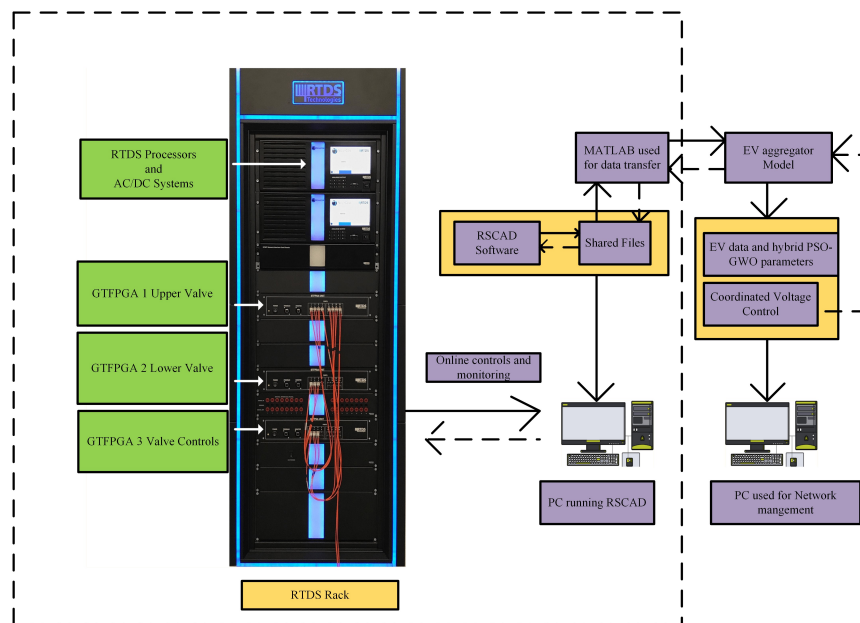


Figure 3. Real time digital simulation (RTDS Technologies NovaCor Model-1A) arrangement with MATLAB 2022a for overall solution procedure of IEEE-37 node microgrid.

evaluated through IEEE-37 node feeder (medium scale microgrid) using RTDS to determine its overall performance. An EV aggregator participates in and solves the optimal scheduling problem using RTDS. AC/DC Microgrid has been classified into small-scale and medium-scale category based on factors such as generation capacity, demand and evaluation time.

In this research, we focus on microgrid operating in grid-connected and islanded mode, where the collective output of available generation sources expects to meet the demand every hour. Islanded mode entails that the microgrid meets its demand using renewable energy sources and Combined Heat and Power (CHP). We employ a cost-effective hybrid PSO-GWO algorithm to optimize the distribution of demand power among diverse DERs. The algorithm prioritizes efficient power allocation among available sources to minimize generation costs while ensuring load satisfaction. The proposed cost-effective hybrid PSO-GWO algorithm in comparison with other algorithms has been implemented for small scale and medium-scale AC/DC microgrids. A set of 100 EVs for charging/discharging mode are considered

for the V2G and G2V framework with 30 EVSEs. The parameter setting for the hybrid PSO-GWO is to calculate the scheduling time for the EVs during peak and off-peak hours with 40 KW battery rated capacity. The optimal solution for scheduling EV for charging/discharging has been carried out using MATLAB 2022a and the time for computing the total path is 0.170 seconds. To find the nearest EV parking system for charging, the Poisson distribution function has been used for hybrid PSO-GWO. It has been observed that each EV requires 30 minutes for full charging. Each EV travels at a speed of 50 km/hour and has touch screen panels for checking the SOC. If $SOC_{EV} < SOC_{BDT}$, then the EV will move for charging and if the $SOC_{EV} > SOC_{BDT}$, then the EV will be in discharged mode. The designed data will be operated in terms of travel frequency, duration per trip, starting time of the trip and driving mileage per trip [46] for V2G and G2V scenario (as shown in Fig. 4) by evaluating its performance in real time environment. The generation data and all algorithms were tested using the same dataset for fair comparison in terms of cost optimization. Results demonstrate that the proposed hybrid PSO-GWO algorithm

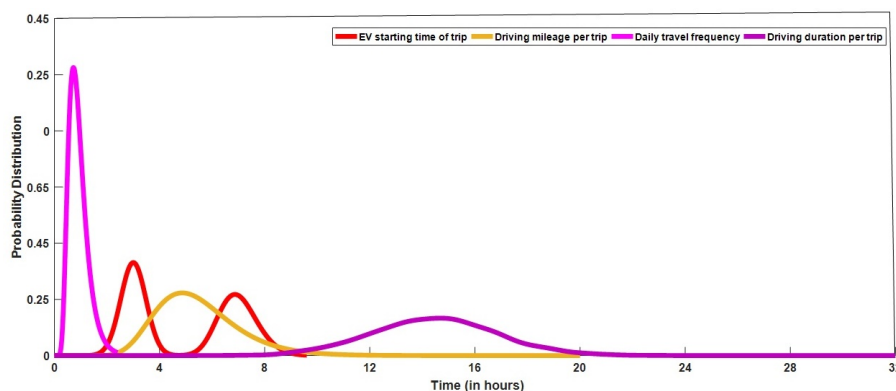


Figure 4. EV charging/discharging travelling analysis using hybrid PSO-GWO.

outperforms other investigated meta-heuristic algorithms. Each algorithm underwent 60 runs for a 24 h load dataset with unbiased evaluation for obtaining the best optimized cost. Uniform population size and maximum iteration numbers were maintained across all algorithms for consistency, while other parameters were adjusted as per microgrid standards. The parameter settings of all algorithms such as

universe size, learning factors, crossover/mutation probabilities and inertia weights have been chosen based on convergence speed, robustness and stability which impacts convergence efficiency, system performance and solution accuracy in managing load and DERs in microgrids as provided in Table 2.

The medium scale microgrid configurations are described in

Table 2. Parameter settings of all algorithms, DERs capacity quantities and load data (in KW) for medium scale.

Algorithm	Parameter	Value	DERs	Capacity	Hour	Load (KW) IEEE 37 (medium scale microgrid)
hybrid PSO-GWO	universe size	60	EV rated power	275 KW	1	1771
	number of iterations	1500	EV rated capacity	85 KWh	2	1625
	explorations & exploitation	0.8 to 0.3	controller parameter – EV		3	1563
	learning factor	2	droop coefficient	$R_{Droop} = 0.06$, $D_p = 1 \times 10^{-3}$	4	1529
	inertia weight	0.8 to 0.3	voltage controller	$K_p^{EVV} = 3.68$, $K_I^{EVV} = 181.08$	5	1529
PSO	universe size	60	current controller	$K_p^{EVc} = 0.157$, $K_I^{EVc} = 19.5$	6	1621
	number of iterations	1500	IC-VSC		7	1809
	learning factor	2	droop coefficient	$D_p^{IC} = 1.5708 \times 10^{-4}$, $D_Q^{IC} = 1.7 \times 10^{-3}$	8	1963
	inertia weight	0.8 to 0.3	power controller	$K_p^{IC} = 2 \times 10^{-5}$, $K_d^{IC} = 2 \times 10^{-7}$	9	1957
GWO	universe size	60	voltage controller	$K_p^{IC} = 0.11$, $K_I^{IC} = 2.2$	10	1943
	number of iterations	1500	current controller	$K_p^{IC} = 0.16$, $K_I^{IC} = 200$	11	1952
	explorations & exploitation	0.8 to 0.3	filter parameter		12	1966
GA	universe size	60	IC VSC	$L_f = 10mH$, $C_f = 400\mu F$, $C_{DC} = 13000\mu F$	13	1939
	number of iterations	1500	PV boost converter	$L_f = 8mH$, $C_{DC} = 5000\mu F$	14	1942
	crossover probability	0.8	EV converter	$L_f = 10mH$, $C_{DC} = 1000\mu F$	15	1940
	mutation probability	0.4	line parameter		16	1976
MVO	universe size	60	line parameter of AC DER	$R_{lder1\&2} = 0.0075\Omega$, $L_{lder1\&2} = 0.15mH$	17	2220
	number of iterations	1500	line parameter of IC VSC	$R_L^{IC} = 0.015$, $L_L^{IC} = 0.00175$	18	2514
	Min	0.2	line parameter of PV	$R_L^{PV} = 0.0025\Omega$	19	2682
	Max	1	line parameter of EV	$R_L^{EVref} = 0.001$ to 0.05	20	2682
	P	6	line parameter for BESS	$R_L^{BESS} = 0.001$	21	2627
CMVO	universe size	60			22	2474
	number of iterations	1500			23	2203
	WEP	0.3			24	2682
AHA	universe size	60				
	number of iterations	1500				
	migration coefficient	2n				

Table 3. The data set parameter has been tested for medium-scaled IEEE-37 node test feeder. The capacities of all DERs integrated with the microgrid have been described in Table 2 with IC-VSC, controller, filter and line coefficients quantities.

4.2 Medium scale microgrid experimental results

This microgrid comprises three wind plants, two PV plants, one CHP system and EVs. The load area is modeled for IEEE 37-bus test system as illustrated in Table 3. The generation and load data for this microgrid has WPP of 750 KW, PV plant of 650 KW, CHP of 1000 KW and single EV as 275 KW rated capacities. The wind and PV plants exhibit intermittent output, varying their power generation each hour, whereas the CHP system maintains a consistent output throughout the day. In this analysis, we assume the generation sources which maintain the continuous operation by enabling the microgrid to function independently in islanded mode without depending on the main grid.

The wind and PV plants are characterized by their intermittent nature which results in varying power outputs every hour. In contrast, the CHP system consistently provides the same amount of power throughout the day. This analysis assumes continuous operation of the generation sources, ensuring the microgrid functions independently in islanded mode without reliance on the main grid. The load dataset for medium scale microgrid is detailed in Table 2 and the cost coefficients for medium scale microgrid has been described in Table 3.

In the experimental results, the performance of medium scale microgrid is elucidated based on evaluation time and reduced generation and EV charging costs. These results are derived from medium scale microgrid, each with their corresponding dataset and initialized parameters. Each algorithm underwent 1500 iterations and the optimal outcomes were selected for a comprehensive and unbiased evaluation. This section delves into the optimization results for medium scale microgrid which employs seven different metaheuristic algorithms on the provided dataset. We are assuming that the generated power consistently meets the demanded power by satisfying the equality constraint. Table 4 showcases the hourly generation power of all seven DERs - WP1,

WP2, WP3, PV1, PV2, CHP and EVs. The load data pertinent to this microgrid is outlined in Table 2. The Table 4 presents the outcomes derived from the GWO detailing the generation power of all DERs with total generation cost of \$1292.51. Table 4 displays the results obtained through PSO showing a total generation cost of \$1317.99. Table 5 and Table 6 delve into the generation power outputs for MVO algorithm with total generation cost is recorded as \$1376.11 and \$1352.59 for CMVO, \$1407.71 for AHA and for GA \$1391.87 respectively. Table 7 delves the overall generation cost of our proposed algorithm hybrid PSO-GWO with \$1255.24. These tables offer a comparative view of various algorithms employed for the optimal power scheduling of all available generation units within the hour, shedding light on their respective performance in achieving cost-effective and efficient solutions for medium scale microgrid.

Table 8 illustrates the total generation cost resulting from optimal power scheduling across various available DERs, as implemented for different algorithms. From the data in Table 8, it becomes evident that the hybrid PSO-GWO algorithm demonstrates remarkably improved results i.e., \$1255.24. This algorithm achieves optimal scheduling at a lower cost compared to all other algorithms studied. Specifically, the total costs incurred by CMVO, MVO, PSO, AHA, GA and GWO amount to \$1352.59, \$1376.11, \$1317.99, \$1407.71, \$1391.87 and \$1292.51 respectively. This analysis reveals varying degrees of daily cost reduction, ranging from \$10.05 to \$152.47 in comparison with all metaheuristic algorithms. Furthermore, the average time taken by each algorithm per hour differs significantly: hybrid PSO-GWO at 0.21 s, CMVO at 0.29 s, MVO at 0.36 s, PSO at 0.34 s, AHA at 0.88 s, GA at 0.65 s and GWO at 0.24 s. In Table 8, the mean and standard deviation for each algorithm is detailed. This finding suggests that the proposed algorithm is not only more stable but also more cost-effective than the other algorithms under investigation.

Fig. 5 depicts the convergence graph for the 12th hour which highlights the optimal outcomes across all operating hours. This graph illustrates the efficient convergence of the proposed algorithm by exploring the search space. The convergence graph plots the best solution against the generation iteration number.

Table 3. Medium scale microgrid configurations and cost coefficients.

microgrid 1		Plant	α	β	δ
IEEE test system	IEEE 37-node test feeder		medium scale microgrid		
scale	medium	WP1	0.0026	16.82	4.47
no. of solar plants	2	WP2	0.0027	17.41	4.46
no. of wind plants	3	WP3	0.0025	17.32	4.45
no. of CHP	1	PV1	0.0054	28.32	4.47
		PV2	0.0054	28.91	4.47
		CHP	0.0082	74.71	5.28
		V2G	0.0060	36.80	4.91

Table 4. Generation power (in KW) by GWO and PSO individually for medium scale microgrid.

hour	WP1		WP2		WP3		PV1		PV2		CHP		V2G		cost (\$)	
	GWO	PSO	GWO	PSO	GWO	PSO	GWO	PSO	GWO	PSO	GWO	PSO	GWO	PSO	GWO	PSO
1	400.62	401.64	300.21	301.23	276.62	277.64	280.21	281.23	0	0	262.96	264.98	10.21	11.23	39.17	40.19
2	399.98	401.00	250.52	251.54	230.98	232.00	250.92	251.94	0	0	205.23	206.25	30.22	25.24	32.91	33.93
3	209.21	210.23	220.24	221.26	210.01	211.03	220.21	221.23	0	0	189.12	190.14	9.18	10.20	31.51	32.53
4	200.43	201.45	196.45	197.47	195.43	196.45	200.45	201.47	0	0	198.96	200.98	09.21	10.23	30.05	31.07
5	184.58	185.60	196.45	197.47	195.43	196.45	200.45	201.47	0	0	198.96	200.98	12.21	13.23	36.86	37.88
6	230.98	232.00	247.92	248.94	230.98	232.00	250.92	251.94	0	0	215.23	216.25	0	0	39.48	40.50
7	214.98	216.00	248.65	249.67	230.98	232.00	250.92	251.94	0	0	225.23	226.25	0	0	42.48	43.50
8	500.25	501.27	500.68	501.70	310.33	311.35	310.98	312.00	0	0	288.69	289.71	0	0	47.97	49.99
9	500.38	501.40	500.90	501.92	300.34	301.36	280.90	281.92	0	0	290.21	291.23	0	0	42.39	43.41
10	521.01	522.03	499.25	500.27	285.32	286.34	286.22	287.24	0	0	285.21	286.23	0	0	42.25	43.27
11	486.23	487.25	487.87	489.89	300.34	301.36	280.90	281.92	0	0	268.21	269.23	0	0	48.25	49.27
12	305.30	306.32	325.67	326.69	310.30	311.32	316.62	317.64	0	0	315.48	316.50	0	0	49.98	51.00
13	0	1.02	599.43	600.45	288.43	289.45	316.43	317.45	0	0	316.69	317.71	0	0	50.25	51.27
14	279.33	280.35	482.20	483.22	288.33	289.35	306.80	307.82	24.30	25.32	315.23	316.25	0	0	51.85	52.87
15	266.32	267.34	478.32	479.34	268.32	269.34	306.98	308.00	0	0	316.12	317.14	0	0	52.65	53.67
16	268.21	269.23	465.32	466.34	288.21	289.23	316.98	318.00	36.87	37.89	317.21	318.23	0	0	68.21	69.23
17	310.53	311.55	487.32	488.34	310.33	311.35	386.90	387.92	39.24	40.26	312.32	313.34	0	0	72.96	73.98
18	299.23	300.25	423.82	424.84	310.23	311.25	586.98	588.00	48.17	49.19	517.26	518.28	0	0	82.25	83.27
19	300.33	301.35	599.32	600.34	320.33	321.35	600.90	601.92	0	0	516.62	517.64	0	0	81.92	82.94
20	405.35	406.37	200.25	201.27	340.63	341.65	600.98	602.00	0	0	616.52	617.54	0	0	75.74	76.76
21	469.25	470.27	478.52	479.54	481.33	482.35	476.89	477.91	0	0	481.33	482.35	0	0	76.25	77.27
22	418.66	419.68	409.65	410.67	426.66	427.68	423.76	424.78	0	0	429.22	430.24	0	0	77.25	78.27
23	276.33	277.35	301.87	302.89	288.33	289.35	306.80	307.82	0	0	316.69	317.71	4.52	5.54	64.25	65.27
24	513.98	515.00	479.09	480.11	533.98	535.00	490.21	491.23	0	0	421.86	422.88	5.58	6.60	55.63	56.65

Table 5. Generation power (in KW) by MVO and CMVO for medium scale microgrid.

hour	WP1		WP2		WP3		PV1		PV2		CHP		V2G		cost (\$)	
	MVO	CMVO	MVO	CMVO	MVO	CMVO	MVO	CMVO	MVO	CMVO	MVO	CMVO	MVO	CMVO	MVO	CMVO
1	403.86	402.88	303.45	302.47	279.86	278.88	283.45	282.47	0	0	267.20	266.22	13.45	12.47	42.41	41.43
2	403.22	402.24	253.76	252.78	234.22	233.24	254.16	253.18	0	0	208.47	207.49	33.46	28.48	36.15	35.17
3	212.45	211.47	223.48	222.50	213.25	212.27	223.45	222.47	0	0	192.36	191.38	12.42	11.44	34.75	33.77
4	203.67	202.69	199.69	198.71	198.67	197.69	203.69	202.71	0	0	203.20	202.22	12.45	11.47	33.29	32.31
5	187.82	186.84	199.69	198.71	198.67	197.69	203.69	202.71	0	0	203.20	202.22	15.45	14.47	40.10	39.12
6	234.22	233.24	251.16	250.18	234.22	233.24	254.16	253.18	0	0	218.47	217.49	0	0	42.72	41.74
7	218.22	217.24	251.89	250.91	234.22	233.24	254.16	253.18	0	0	228.47	227.49	0	0	45.72	44.74
8	503.49	502.51	504.92	503.94	313.57	312.59	314.22	313.24	0	2.26	291.93	290.95	0	0	52.21	51.23
9	503.62	502.64	504.12	503.14	303.58	302.60	284.12	283.14	0	2.98	293.45	292.47	0	0	46.63	45.65
10	524.25	523.27	502.49	501.51	288.56	287.58	289.46	288.48	0	0	288.45	287.47	0	0	46.47	45.49
11	489.47	488.49	492.11	491.13	303.58	302.60	284.12	283.14	0	2.26	271.45	270.47	0	0	52.47	51.49
12	308.54	307.56	328.91	327.93	313.54	312.56	319.86	318.88	0	2.26	318.72	317.74	0	0	54.20	53.22
13	3.24	2.26	602.67	601.69	291.67	290.69	319.67	318.69	3.24	0	319.93	318.95	0	0	54.49	53.51
14	282.57	281.59	485.44	484.46	291.57	290.59	310.04	309.06	27.54	26.56	318.47	317.49	0	0	55.09	54.11
15	269.56	268.58	481.56	480.58	271.56	270.58	310.22	309.24	0	2.26	319.36	318.38	0	0	55.89	54.91
16	271.45	270.47	468.56	467.58	291.45	290.47	320.22	319.24	40.11	39.13	320.45	319.47	0	0	71.45	70.47
17	313.77	312.79	490.56	489.58	313.57	312.59	390.14	389.16	42.48	41.50	315.56	314.58	0	0	76.20	75.22
18	302.47	301.49	427.06	426.08	313.47	312.49	590.22	589.24	51.41	50.43	520.50	519.52	0	0	85.49	84.51
19	303.57	302.59	602.56	601.58	323.57	322.59	604.14	602.16	0	2.28	519.86	519.88	0	0	85.16	84.18
20	408.59	407.61	203.47	202.49	343.87	342.89	605.22	603.24	0	0	619.76	618.78	0	0	78.96	77.98
21	472.49	471.51	481.76	480.78	484.57	483.59	480.13	479.15	0	0	484.57	483.59	0	0	79.47	78.49
22	421.90	420.92	412.89	411.91	429.90	428.92	426.00	425.02	0	0	432.46	431.48	3.24	0	80.47	79.49
23	279.57	278.59	304.11	303.13	291.57	290.59	309.04	308.06	0	0	319.93	318.95	7.76	6.78	67.47	66.49
24	517.22	516.24	482.33	481.35	537.22	536.24	493.45	492.47	0	0	425.10	424.12	8.82	7.84	58.85	57.87

Table 6. Generation power (in KW) by AHA and GA for medium scale microgrid.

hour	WP1		WP2		WP3		PV1		PV2		CHP		V2G		cost (\$)	
	AHA	GA	AHA	GA	AHA	GA	AHA	GA	AHA	GA	AHA	GA	AHA	GA	AHA	GA
1	405.01	407.85	304.60	307.44	281.01	283.85	284.60	287.44	0	7.20	268.35	271.19	14.60	17.44	43.56	46.40
2	404.37	407.21	254.91	257.75	235.37	238.21	255.31	258.15	0	6.98	209.62	212.46	24.61	27.45	37.30	40.14
3	213.60	216.44	224.63	227.47	214.40	217.27	224.60	227.44	0	7.22	193.51	196.35	13.57	16.41	36.90	38.74
4	204.82	207.66	200.84	203.68	199.82	202.66	204.84	207.68	0	7.34	204.35	207.19	13.60	16.44	35.44	37.28
5	188.97	191.81	200.84	203.68	199.82	202.66	204.84	207.68	0	7.32	204.35	207.19	16.60	19.44	41.25	44.09
6	235.37	238.21	252.31	255.15	235.37	238.21	255.31	258.15	0	6.95	219.62	222.46	0	0	44.87	46.71
7	219.37	222.21	252.04	255.88	235.37	238.21	255.31	258.15	0	7.54	229.62	232.46	0	0	47.87	49.71
8	504.64	507.48	506.07	508.91	314.72	317.56	315.37	318.21	0	7.34	293.08	295.92	0	0	53.36	56.20
9	504.77	507.61	505.27	508.11	304.73	307.57	285.27	288.11	0	7.78	294.60	297.44	0	0	47.78	50.62
10	525.40	528.24	503.64	506.48	289.71	292.55	290.61	293.45	0	7.89	289.60	292.44	0	0	47.62	50.46
11	490.62	493.46	493.26	496.10	304.73	307.57	285.27	288.11	0	7.98	272.60	275.44	0	0	53.62	56.46
12	309.69	312.53	330.06	332.90	315.69	317.53	321.01	323.85	0	7.21	319.87	322.71	0	0	55.35	58.19
13	4.39	7.23	603.82	606.66	292.82	295.66	320.82	323.66	0	7.98	321.08	323.92	0	0	55.64	58.48
14	283.72	286.56	486.59	489.43	292.72	295.56	311.19	314.03	28.69	31.53	319.62	322.46	0	0	56.24	59.08
15	270.71	273.55	482.71	485.55	272.71	275.55	311.37	314.21	4.39	7.23	320.51	323.35	0	0	57.04	59.88
16	272.60	275.44	469.71	472.55	292.60	295.44	321.37	324.21	41.26	44.10	321.60	324.44	0	0	72.60	75.44
17	314.92	317.76	491.71	494.55	314.72	317.56	391.29	394.13	43.63	46.47	316.71	316.84	0	0	77.35	80.19
18	303.62	306.46	428.21	431.05	314.62	317.46	591.37	594.21	52.56	55.40	521.65	524.49	0	0	86.64	89.48
19	304.72	307.56	603.71	606.55	324.72	327.56	605.29	607.13	0	7.09	521.01	524.85	0	0	86.31	89.15
20	409.74	412.58	204.62	207.46	345.02	347.86	605.37	608.21	0	7.98	620.91	623.75	0	0	80.11	82.95
21	473.64	476.48	482.91	485.75	485.72	488.56	481.28	484.12	0	7.20	485.72	488.56	0	0	80.62	83.46
22	423.05	426.89	414.04	416.88	431.05	433.89	427.15	429.99	0	7.98	433.61	436.45	0	0	81.62	84.46
23	280.72	283.56	305.26	308.10	292.72	295.56	310.19	312.03	0	7.56	320.08	323.95	8.91	11.75	68.62	71.46
24	518.37	521.21	483.48	486.32	538.37	540.21	494.60	497.44	4.39	7.45	426.25	429.09	10.97	12.81	60.00	62.84

Table 7. Generation power (in KW) by hybrid PSO-GWO for medium scale microgrid.

hour	WP1	WP2	WP3	PV1	PV2	CHP	V2G	cost(\$)
1	397.39	296.98	273.39	276.98	0	259.73	7.98	35.94
2	396.75	247.29	227.75	247.69	0	202.00	25.99	29.68
3	206.98	217.01	206.78	217.98	0	185.89	5.95	28.28
4	197.20	193.22	192.20	197.22	0	195.73	5.98	26.82
5	181.35	193.22	192.20	197.22	0	195.73	9.98	33.63
6	227.75	244.69	227.75	247.69	0	212.00	0	36.25
7	211.75	245.42	227.75	247.69	0	222.00	0	39.25
8	497.02	497.45	307.10	307.75	0	285.46	0	44.74
9	497.15	497.67	297.11	277.67	0	287.98	0	39.16
10	517.78	496.02	282.09	283.99	0	282.98	0	39.02
11	483.00	484.64	297.11	277.67	0	265.98	0	45.02
12	302.07	322.44	307.07	313.39	0	312.25	0	46.75
13	0	596.20	285.20	313.20	0	313.46	0	47.02
14	276.10	479.97	285.10	303.57	21.07	312.00	0	48.62
15	263.09	475.09	265.09	303.75	0	312.89	0	49.42
16	265.98	462.09	285.98	313.75	33.64	313.98	0	65.98
17	307.30	484.09	307.10	383.67	36.01	309.09	0	69.73
18	296.00	420.59	307.00	583.75	44.94	514.03	0	79.02
19	297.10	596.09	317.10	597.67	0	513.39	0	78.69
20	402.12	197.02	337.40	597.75	0	613.29	0	72.51
21	466.02	475.29	478.10	473.66	0	478.10	0	73.02
22	415.43	406.42	423.43	420.53	0	425.99	0	74.02
23	273.10	298.64	285.10	303.57	0	313.46	1.29	61.02
24	510.75	475.86	534.75	487.98	0	418.63	2.35	52.40

This performance surpasses all other algorithms in terms of efficiency and accuracy, which swiftly moves towards a more promising region in fewer generations which yields superior results.

Table 8. Total evaluation time and the total cost for medium scale microgrid.

algorithm	total cost	total time	mean	standard deviation
hybrid PSO-GWO	1255.24	0.21	1299.12	21.28
CMVO	1352.59	0.29	1398.25	38.45
MVO	1376.11	0.36	1421.65	40.54
PSO	1317.99	0.34	1362.17	36.24
GWO	1292.51	0.24	1301.25	23.24
GA	1391.87	0.65	1530.50	44.36
AHA	1407.71	0.88	1682.65	47.65

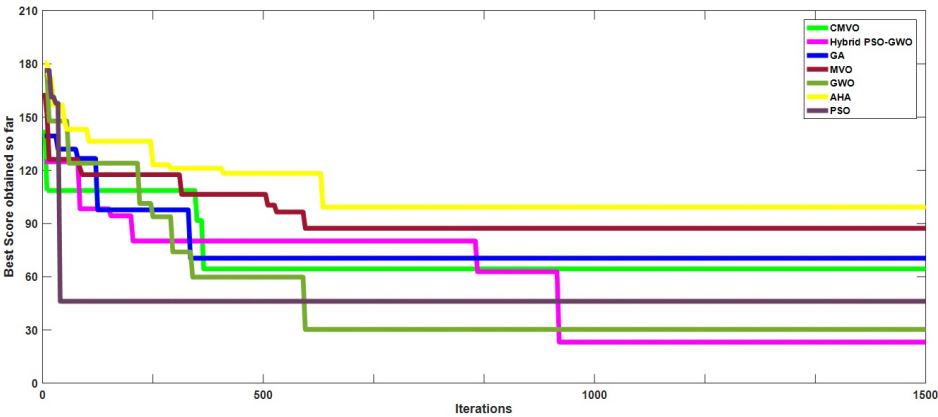


Figure 5. Convergence graphs for medium scale microgrid at 12th hour.

Table 9 and Fig. 6 discusses the EV charging best costs graph for medium scale microgrid in which the proposed hybrid PSO-GWO algorithm outperforms all other meta-heuristic algorithms by obtaining reduced charging cost. The best EV charging cost obtained through hybrid PSO-GWO is \$70.36 for EV as compared to PSO, GWO, MVO, CMVO, AHA and GA. Also, algorithm navigate the best search space and converges towards optimal solutions by demonstrating its potential for superior performance in real time environment.

The generation data for a medium-scale microgrid optimizes through the hybrid PSO-GWO algorithm which highlights the efficacy of strategic power scheduling across various DERs. Table 7 delineates the hourly generation outputs for

wind power (WP1, WP2, WP3), photovoltaic sources (PV1, PV2), CHP and V2G systems, along with the corresponding operational costs per hour for hybrid PSO-GWO. The data shows a judicious distribution of energy resources aimed at cost minimization. The algorithm proficiently directs fluctuations in RE parameters such as variations in wind speed and solar irradiance by merging the exploratory strengths of PSO with the exploitation precision of GWO facilitating dynamic adaptations to sustain cost-efficient operations. However, despite its inherent flexibility, the algorithm may encounter challenges including heightened sensitivity and premature convergence with respect to parameter configuration, which hinders the scalability and compromises real-time performance swiftly with changing conditions. During

Table 9. EV charging best optimized cost for medium scale microgrid.

iterations (1-1000)/ algorithms	MVO	AHA	GA	PSO	CMVO	GWO	hybrid PSO-GWO
iteration 300	\$110.25	\$70.56	\$87.94	\$90.42	\$59.50	\$100.25	\$70.36
iteration 600	\$61.25	\$64.98	\$64.87	\$55.65	\$59.50	\$40.28	\$30.01
iteration 900	\$61.25	\$63.35	\$64.87	\$55.65	\$59.50	\$40.28	\$30.01
iteration 1200	\$61.25	\$62.50	\$60.22	\$55.65	\$59.50	\$40.28	\$30.01
iteration 1500	\$61.25	\$62.50	\$60.22	\$55.65	\$59.50	\$40.28	\$30.01

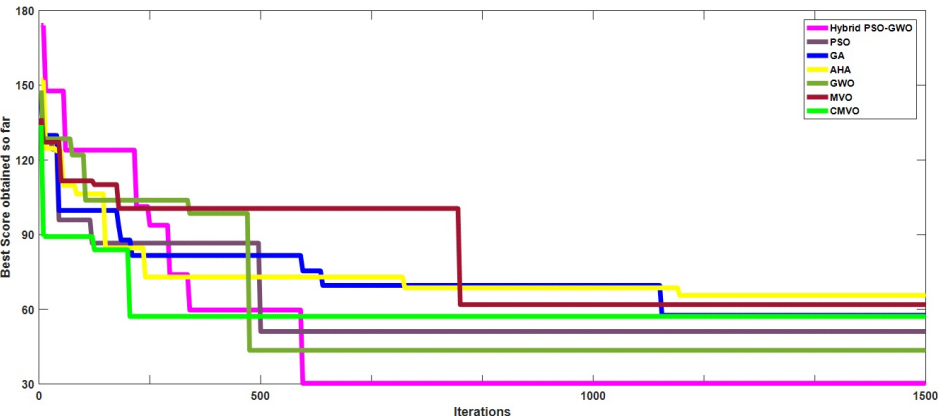


Figure 6. Best EV charging costs for medium scale microgrid.

peak generation periods i.e., 8thh and 9thh when wind and PV outputs are at their highest, the system influences these sources predominantly, supplemented by V2G operation when needed. During lower generation intervals i.e., 1sth to 5thh, dependence on CHP and V2G systems intensifies leading to elevated costs due to reduced renewable input. The hybrid PSO-GWO algorithm while proficient at optimizing EV charging/discharging costs within microgrids is not without its limitations. It is prone to premature convergence because of its extremely sensitive way of parameter selection and faces scalability challenges as the problem size expands which can impede its ability to thoroughly explore the solution space and adapt effectively to rapid fluctuations in grid conditions. Moreover, computational time for larger-scale applications may become a significant block in real-time approaches. The major perceptions from the data include the sustained deployment of CHP to uphold grid stability during diminished RE generation and the tactical engagement of the V2G system during specific hours to fine-tune costs and enhance charging/discharging efficacy. The hourly cost varies significantly with a low of \$26.82 at 4thh and a high of \$79.02 at 18thh reflecting the intricate balance between generation and consumption managed by the microgrid. These findings emphasize the hybrid PSO-GWO algorithm capability to optimize power generation and costs effectively, while pointing out the areas where further optimization approaches could mitigate peak costs and reinforce overall system performance.

5. Conclusion

This paper presents the hybrid PSO-GWO algorithm, designed to optimize power allocation in medium-scale microgrid enhancing both global and local search efficiencies. By combining the exploration strengths of PSO with the exploitation abilities of GWO, the algorithm minimizes generation and EV charging/discharging costs considerably improving microgrid efficiency. It also incorporates a comprehensive EV scheduling framework, strengthening system reliability and operational efficacy. The real-time functionality is rigorously validated through extensive testing, where the EV controller continuously monitors DC bus voltage and load profiles, eliminating the need for auxiliary battery energy storage systems (BESS) and reducing operational complexity. A comparative analysis confirms the superiority of the hybrid PSO-GWO algorithm particularly in V2G and G2V scenarios with hourly costs fluctuating between \$26.82 and \$79.02, demonstrating effective management of generation and consumption. The algorithm is highly adaptable across various microgrid configurations and complies with IEEE standards for both islanded and grid-connected systems. Future integration of AI and machine learning will enhance scheduling optimization, while hybridization with other algorithms and multi-objective optimization will improve scalability and efficiency. The PSO-GWO algorithm has transformative potential for smart grids and urban energy networks.

Acknowledgment

Thanks to Jamia Millia Islamia, New Delhi for their assistance for data collection and technical reports for

reference.

Authors contributions

Authors have contributed equally in preparing and writing the manuscript.

Availability of data and materials

The data that support the findings of this study are available from the corresponding author upon reasonable request.

Conflict of interests

The authors declare that they have no known competing financial interests or personal relationships that could have appeared to influence the work reported in this paper.

Nomenclature

Index terms		Abbreviations	
I_{PV_cell}	current output of a single PV array model	EV	Electric Vehicle
I_{pg}	photogenerated current	PSO	Particle Swarm Optimization
I_{Rev}	reverse current	GWO	Grey Wolf Optimization
η	ideality factor	I-VSC	Interleaved Voltage Source Converter
$R_s \& R_p$	series resistance and shunt resistance	IC-VSC	Interline Cascade Voltage Source Converter
V_{MPPT}, I_{MPPT}	maximum power point voltage and current	DESS	Distributed Energy Storage System
$\omega_{inst}, \omega_{ref}$	instantaneous and reference frequency in rad/sec	IEEE	Institute of Electrical and Electronics Engineers
K_{PC}^{IC}	IC-VSC proportional coefficient power control loop	SA	Simulated Annealing
K_d^{IC}	derivative coefficient in power control loop at grid converter side	DER	Distributed Energy Resources
V_d^{ref}, V_q^{ref}	reference voltage control loop for d-q component	RES	Renewable Energy Sources
K_{PV}^{IC}	IC-VSC voltage control loop	RER	Renewable Energy Resources
C_f	capacitive frequency	ML	Machine Learning
V_d	Voltage at direct axis	AI	Artificial Intelligence
V_q	voltage at quadrature axis	RTDS	Real Time Digital Simulator
K_i	integral IC-VSC constant	RSCAD	Real-time Simulation Computer Aided Design
$V_{DC}^{rated}, V_{DC}^{inst}$	rated and instantaneous DC bus voltage	PV	PhotoVoltaic
K_P^{SC}, K_i^{SC}	proportional and integral coefficients of secondary controller	WPP	Wind Power Plant
P_{min}	minimum power generated in WPP	CHP	Combined Heat and Power
P_{max}	maximum power	ESS	Energy Storage system
$P_{CHP,elec}$	maximum electricity generation capacity in CHP	BEES	Battery Energy Storage System
σ	driving efficacy during EV charging/discharging	CES	Conventional Energy Sources
M	distance travelled by EV per trip	RE	Renewable Energy
M_{max}	maximum distance travelled by the EV for the whole day	EVSE	Electric Vehicle Supply Equipment
SOC_{ch}^{EV}	SOC during EV charging	CS	Charging Station
SOC_{disch}^{EV}	SOC during EV discharging	ACS	Advanced Control Systems
SOC_I^{EV}	EVs initial stage	V2G	Vehicle-To-Grid
C_{ch} and C_{disch}	EV battery charging/discharging efficacy and its performance	G2V	Grid-To-Vehicle
ϵ_{ch} and ϵ_{disch}	EV charging/discharging rate	ANN	Artificial Neural Networks

Index terms		Abbreviations	
$T_{ch}^{EV}, T_{disch}^{EV}$	dedicated scheduling for EV charging/discharging process	MOA	Mayfly Optimization Algorithm
$V_{DC}^{inst.Bus}, V_{DC}^{ref}$	DC bus instantaneous and reference voltage	LSA	Lightning Search Algorithm
D_p	power droop coefficient	RFA	Rain Flow Algorithm
$K_P^{EV^C}, K_i^{EV^C}$	proportional and integral coefficient in current control loop for EV converter	MILP	Mixed Integer Linear Programming
I_{PV_cell}	current output of a single PV array model	EV	Electric Vehicle
$\beta_j, \alpha_j, \delta_j$	cost coefficients of the microgrid	MDP	Markov Decision Process
C_j	total cost	MVO	multi-verse optimization
P_j	power in j^{th} generation in MW/hour	GA	Genetic Algorithm
P_i	total power generated from available DERs	DR	Demand Response
P_t	power demanded at a particular hour of the day	WT	Wind Turbine
$P_{i \min}$	minimum allowable power output for any generation unit	DG	Distributed Generation
$P_{i \max}$	the maximum power output or total demand achievable based on the rated power capacity	TLBO	Teaching Learning-Based Optimization
SOC_i	SOC of EV at i^{th} iteration	SOC	State-Of-Charge
W_t	mean waiting time	MPPT	Maximum Power Point Tracking
Z_α	alpha wolf	EM	Energy Management
Z_β	beta wolf	JA	Jaya Algorithm
Z_δ	delta wolf	DSO	Distributed System Operator

References

- [1] A. Saif, R. V. Pandit, H. H. Zeineldin, and S. Kennedy. "Optimal allocation of distributed energy resources through simulation-based optimization". 104:1–8, 2018.
DOI: <https://doi.org/10.1016/j.ejpsr.2013.05.019>.
- [2] A. Askarzadeh. "A memory-based genetic algorithm for optimization of power generation in a microgrid". *IEEE Trans. Sustain. Energy*, 9:1081–1089, 2018.
DOI: <https://doi.org/10.1109/TSTE.2017.2765483>.
- [3] M. Uddin, H. Mo, D. Dong, S. Elsayah, J. Zhu, and M. J. Guerrero. "Microgrids: A review, outstanding issues and future trends.". *Energy Strategy Reviews*, 49:101127, 2023.
DOI: <https://doi.org/10.1016/j.esr.2023.101127>.
- [4] M. Abbasi, E. Abbasi, L. Li, R. P. Aguilera, D. Lu, and F. Wang. "Review on the microgrid concept, structures, components, communication systems and control methods.". *Energies*, 16:484, 2023.
DOI: <https://doi.org/10.3390/en16010484>.
- [5] D. Said and H. T. Mouftah. "A novel electric vehicles charging/dis-charging management protocol based on queuing model". *IEEE Trans. Intell. Vehicles*, 5:1–10, 2020.
DOI: <https://doi.org/10.1109/TIV.2019.2955370>.
- [6] K. Gholami and E. Dehnavi. "A modified particle swarm optimization algorithm for scheduling renewable generation in a micro-grid under load uncertainty.". *Appl. Soft Comput.*, 78:496–514, 2019.
DOI: <https://doi.org/10.1016/j.asoc.2019.02.042>.
- [7] F. M. Roslan, A. M. Hannan, J. P. Ker, A. R. Begum, I. T. Mahlia, and Y. Z. Dong. "Scheduling controller for microgrids energy management system using optimization algorithm in achieving cost saving and emission reduction.". *Appl. Energy*, 292:116883, 2021.
DOI: <https://doi.org/10.1016/j.apenergy.2021.116883>.
- [8] A. S. Amamra and J. Marco. "Vehicle-to-grid aggregator to support power grid and reduce electric vehicle charging cost.". *IEEE Access*, 7:178528–178538, 2019.
DOI: <https://doi.org/10.1109/ACCESS.2019.2958664>.
- [9] M. Zhou, Z. Wu, J. Wang, and G. Li. "Forming dispatchable region of electric vehicle aggregation in microgrid bidding". *IEEE Trans. Ind. Informatics*, 17:7–20, 2021.
DOI: <https://doi.org/10.1109/TII.2020.3020166>.
- [10] S. M. Rahman, J. M. Hossain, J. Lu, M. H. F. Rafi, and S. Mishra. "A vehicle-to-microgrid framework with optimization-incorporated distributed EV coordination for a commercial neighbourhood.". *IEEE Trans. Ind. Informatics*, 17, 2020.
DOI: <https://doi.org/10.1109/TII.2019.2924707>.
- [11] Q. Yan, B. Zhang, and M. Kezunovic. "Optimized operational cost reduction for an EV charging station integrated with battery energy storage and PV generation.". *IEEE Trans. Smart Grid*, 10, 2019.
DOI: <https://doi.org/10.1109/TSG.2017.2788440>.
- [12] X. Lu, M. J. Guerrero, K. Sun, C. J. Vasquez, R. Teodorescu, and L. Huang. "Hierarchical control of parallel AC-DC converter interfaces for hybrid microgrids". *IEEE Trans. Smart Grid*, 5, 2014.
DOI: <https://doi.org/10.1109/TSG.2013.2272327>.
- [13] M. J. Guerrero, C. J. Vasquez, J. Matas, D. C. L. Vicuña, and M. Castilla. "Hierarchical control of droop-controlled AC and DC microgrids—A general approach toward standardization.". *IEEE Trans. Ind. Electron.*, 58, 2011.
DOI: <https://doi.org/10.1109/TIE.2010.2066534>.
- [14] S. M. Rahman, J. M. Hossain, and J. Lu. "Coordinated control of three-phase AC and DC type EV-ESSs for efficient hybrid microgrid operations.". *Energy Convers. Manage.*, 122:488–503, 2016.
DOI: <https://doi.org/10.1016/j.enconman.2016.05.070>.
- [15] K. M. Senapati, C. Pradhan, R. S. Samantaray, and K. P. Nayak. "Improved power management control strategy for renewable energy-based DC microgrid with energy storage integration.". *IET Gener., Transm. Distrib.*, 13, 2019.
DOI: <https://doi.org/10.1049/iet-gtd.2018.5019>.
- [16] Y. Bansal and R. Sodhi. "A statistical features based generic passive islanding detection scheme for IIDGs system.". *IEEE Trans. Power Delivery*, 37:3176–3188, 2022.
DOI: <https://doi.org/10.1109/TPWRD.2021.3124986>.
- [17] S. Sharma, M. Amir, A. M. Alotaibi, H. Malik, A. Afthanorhan, and T. S. Ustun. "Optimal control strategies for reliable operation of electric vehicle charging stations under fault tolerant scenarios.". *International Journal of Mathematical, Engineering and Management Sciences*, 9(6):1357–1381, 2024.
DOI: <https://doi.org/10.33889/IJMEMS.2024.9.6.073>.
- [18] N. N. Adnan, S. M. Rahman, I. P. Vasant, and M. A. Noor. "An overview of electric vehicle technology: A vision towards sustainable.". *Green marketing and environmental responsibility in modern corporations*, 216, 2017.
DOI: <https://doi.org/10.4018/978-1-5225-5210-9.ch013>.
- [19] A. M. G. M. Rasol, A. M. Hannan, A. Mohamed, U. A. U. Amirulidin, Z. B. I. Abidin, and N. M. Uddin. "An optimal scheduling controller for virtual power plant and microgrid integration using the binary backtracking search algorithm.". *IEEE Trans. Ind. Appl.*, 54:2834–2844, 2018.
DOI: <https://doi.org/10.1109/TIA.2018.2797121>.
- [20] M. Yilmaz and P. T. Krein. "Review of battery charger topologies, charging power levels, and infrastructure for plug-in electric and hybrid vehicles.". *IEEE Transactions on Power Electronics*, 28:2151–2169, 2013.
DOI: <https://doi.org/10.1109/TPEL.2012.2212917>.
- [21] H. F. Aghdam, T. N. Kalantari, and M. B. Iyatloo. "A chance constrained energy management in multi-microgrid systems considering degradation cost of energy storage elements.". *Journal of Energy Storage*, 29, 2020.
DOI: <https://doi.org/10.1016/j.est.2020.101416>.
- [22] I. S. Bayram, G. Michailidis, M. Devetsikiotis, and F. Granelli. "Electric power allocation in a network of fast charging stations.". *IEEE Journal on Selected Areas in Communications*, 31:1235–1246, 2013.
DOI: <https://doi.org/10.1109/JSAC.2013.130707>.
- [23] O. Berman, R. C. Larson, and N. Fouska. "Optimal location of discretionary service facilities.". *Transportation Science*, 26:201–211, 1992. URL <http://www.jstor.org/stable/25768539>.
- [24] H. Cai, X. Jia, A. S. Chiu, X. Hu, and M. Xu. "Siting public electric vehicle charging stations in Beijing using big-data informed travel patterns of the taxi fleet.". *Transportation Research Part D: Transport and Environment*, 33:39–46, 2014.
DOI: <https://doi.org/10.1016/j.trd.2014.09.003>.
- [25] J. Liu. "Electric vehicle charging infrastructure assignment and power grid impacts assessment in Beijing.". *Energy Policy*, 51:544–557, 2012.
DOI: <https://doi.org/10.1016/j.enpol.2012.08.074>.
- [26] Q. S. Shi and X. Z. Zheng. "Electric vehicle charging stations optimal location based on fuzzy c-means clustering.". *Applied Mechanics and Materials*, pages 556–562, 2014.
DOI: <https://doi.org/10.4028/www.scientific.net/AMM.556-562.3972>.
- [27] M. J. Hodgson. "A flow-capturing location-allocation model.". *Geographical Analysis*, 22:270–279, 1990.
DOI: <https://doi.org/10.1111/j.1538-4632.1990.tb00210.x>.

- [28] M. Manbachi and M. Ordóñez. “AMI-based energy management for islanded AC/DC microgrids utilizing energy conservation and optimization.”. *IEEE Transactions on Smart Grid*, 10:293–304, 2019.
DOI: <https://doi.org/10.1109/TSG.2017.2737946>.
- [29] J. Desjardins. “Visualizing the rise of the electric vehicle.”. 2018. URL <https://www.visualcapitalist.com/riseelectric-vehicle>.
- [30] S. Sharma, I. Ali, and A. M. Aftab. “Demand response mechanism in user-centric markets integrated with electric vehicles.”. *IEEE Delhi Section Conference (DELCON)*, New Delhi, India, pages 1–6, 2022.
DOI: <https://doi.org/10.1109/DELCON54057.2022.9753579>.
- [31] J. Wang, L. M. Costa, , and B. M. Cisse. “From distribution feeder to microgrid: an insight on opportunities and challenges.”. *Proceedings of the IEEE International Conference on Power System Technology (POWERCON 2016)*, Wollongong, Australia, page 28, 2016.
DOI: <https://doi.org/10.1109/POWERCON.2016.7753897>.
- [32] S. Sharma and I. Ali. “Optimized electric vehicle charging and discharging with sporadic renewable energy source.”. *International Conference on Power, Instrumentation, Energy and Control (PIECON)*, Aligarh, India, pages 1–6, 2023.
DOI: <https://doi.org/10.1109/PIECON56912.2023.10085780>.
- [33] I. Ali and S. Sharma. “Design and implementation of energy efficiency augmentation using renewable energy source for small-scaled residential micro-grid.”. *Advances in Energy Technology, Lecture Notes in Electrical Engineering*, Eds. Springer, 766, 2022.
DOI: https://doi.org/10.1007/978-981-16-1476-7_62.
- [34] “Electric Vehicles (EV).”. 2019. URL <http://www.ieso.ca/>.
- [35] P. A. J. Lopes, J. F. Soares, and R. M. P. Almeida. “Integration of electric vehicles in the electric power system.”. *Proceedings of the IEEE*, 19:168–183, 2011.
DOI: <https://doi.org/10.1109/JPROC.2010.2066250>.
- [36] A. K. Barik, S. Jaiswal, and D. C. Das. “Recent trends and development in hybrid microgrid: A review on energy resource planning and control.”. *International Journal of Sustainable Energy*, 41:308–322, 2021.
DOI: <https://doi.org/10.1080/14786451.2021.1910698>.
- [37] A. F. S. Ismail. “DC microgrid planning, operation, and control: A comprehensive review.”. *IEEE Access*, 9:36154–36172, 2021.
DOI: <https://doi.org/10.1109/ACCESS.2021.3062840>.
- [38] S. P. Bihari, P. K. Sadhu, K. Sarita, B. Khan, R. K. Saket, and D. P. Kothari. “A comprehensive review of microgrid control mechanism and impact assessment for hybrid renewable energy integration.”. *IEEE Access*, 9:88942–88958, 2021.
DOI: <https://doi.org/10.1109/ACCESS.2021.3090266>.
- [39] M. Marzband, A. Sumper, J. L. D. García, and R. G. Ferret. “Experimental validation of a real time energy management system for microgrids in islanded mode using a local day-ahead electricity market and MINLP.”. *Energy Conversion and Management*, 76(ISSN 0196-8904):314–322, 2013.
DOI: <https://doi.org/10.1016/j.enconman.2013.07.053>.
- [40] X. Xing, L. Xie, and H. Meng. “Cooperative energy management optimization based on distributed MPC in grid-connected microgrids community.”. *Electrical Power and Energy Systems*, 107: 186–199, 2018.
DOI: <https://doi.org/10.1016/j.ijepes.2018.11.027>.
- [41] Y. E. G. Vera, R. D. Lopez, and J. L. B. Agustin. “Energy management in microgrids with renewable energy sources: A literature review.”. *Applied Sciences*, page 3854, 2019.
DOI: <https://doi.org/10.3390/app9183854>.
- [42] A. A. Askarzadeh. “A memory-based genetic algorithm for optimization of power generation in a microgrid.”. *IEEE Transactions on Sustainable Energy*, 9:1081–1089, 2018.
DOI: <https://doi.org/10.1109/TSTE.2017.2765483>.
- [43] J. Yang, W. Luo, and J. Hou. “Distributed optimal control of AC/DC hybrid microgrid groups with interlinking converters.”. *Journal of Electrical Engineering & Technology*, 2024.
DOI: <https://doi.org/10.1007/s42835-024-01854-3>.
- [44] J. J. Jui, M. A. Ahmad, and M. I. M. Rashid. “Modified multi-verse optimizer for solving numerical optimization problems.”. *Proceedings of the 2020 IEEE International Conference on Automatic Control and Intelligent Systems*, Shah Alam, Malaysia, pages 81–86, 2020.
DOI: <https://doi.org/10.1109/I2CACIS49202.2020.9140097>.
- [45] S. Sharma and I. Ali. “Dynamic pricing strategy for efficient electric vehicle charging and discharging in microgrids using multi-objective jaya algorithm.”. *Engineering Research Express*, 6:035315, 2024.
DOI: <https://doi.org/10.1088/2631-8695/ad6394>.
- [46] E. Espina, R. J. Cárdenas-Dobson, J. W. Simpson-Porco, M. Kaz-erani, and D. Sáez. “A consensus-based distributed secondary control optimization strategy for hybrid microgrids.”. *IEEE Transactions on Smart Grid*, 14(6):4242–4255, 2023.
DOI: <https://doi.org/10.1109/TSG.2023.3263107>.
- [47] S. Sharma and I. Ali. “Efficient energy management and cost optimization using multi-objective grey wolf optimization for EV charging/discharging in microgrid.”. *e-Prime - Advances in Electrical Engineering, Electronics and Energy*, 10(ISSN 2772-6711):100804, 2024.
DOI: <https://doi.org/10.1016/j.prime.2024.100804>.
- [48] C. Berk Saner, J. Saha, and D. Srinivasan. “A social welfare theory-inspired lexicographic optimal charging scheduling framework for modular EV fast charging stations.”. *IEEE Transactions on Intelligent Transportation Systems*, 25(11):18648–18660, 2024.
DOI: <https://doi.org/10.1109/TITS.2024.3451498>.
- [49] K. E. Adetunji, I. W. Hofsaier, A. M. Abu-Mahfouz, and L. Cheng. “A two-tailed pricing scheme for optimal EV charging scheduling using multiobjective reinforcement learning.”. *IEEE Transactions on Industrial Informatics*, 20(3):3361–3370, 2024.
DOI: <https://doi.org/10.1109/TII.2023.3305682>.
- [50] N. Al-Dahabreh et al. “A data-driven framework for improving public EV charging infrastructure: Modeling and forecasting.”. *IEEE Transactions on Intelligent Transportation Systems*, 25(6): 5935–5948, 2024.
DOI: <https://doi.org/10.1109/TITS.2023.3337324>.
- [51] A. Stenstadvolden, O. Stenstadvolden, L. Zhao, M. H. Kapourchali, Y. Zhou, and W. J. Lee. “Data-driven analysis of a NEVI-compliant EV charging station in the Northern Region of the U.S.”. *IEEE Transactions on Industry Applications*, 60(4):5352–5361, 2024.
DOI: <https://doi.org/10.1109/TIA.2024.3397641>.